

Warping model predictive control for application in control of a real airborne wind energy system

Lago, Jesus ; Erhard, Michael; Diehl, Moritz

DOI

[10.1016/j.conengprac.2018.06.008](https://doi.org/10.1016/j.conengprac.2018.06.008)

Publication date

2018

Document Version

Final published version

Published in

Control Engineering Practice

Citation (APA)

Lago, J., Erhard, M., & Diehl, M. (2018). Warping model predictive control for application in control of a real airborne wind energy system. *Control Engineering Practice*, 78, 65-78.
<https://doi.org/10.1016/j.conengprac.2018.06.008>

Important note

To cite this publication, please use the final published version (if applicable).
Please check the document version above.

Copyright

Other than for strictly personal use, it is not permitted to download, forward or distribute the text or part of it, without the consent of the author(s) and/or copyright holder(s), unless the work is under an open content license such as Creative Commons.

Takedown policy

Please contact us and provide details if you believe this document breaches copyrights.
We will remove access to the work immediately and investigate your claim.

Green Open Access added to TU Delft Institutional Repository

'You share, we take care!' – Taverne project

<https://www.openaccess.nl/en/you-share-we-take-care>

Otherwise as indicated in the copyright section: the publisher is the copyright holder of this work and the author uses the Dutch legislation to make this work public.



Warping model predictive control for application in control of a real airborne wind energy system



Jesus Lago^{a,b,*}, Michael Erhard^c, Moritz Diehl^d

^a Delft Center for Systems and Control, Delft University of Technology, The Netherlands

^b Department of Algorithms, Modeling and Optimization, VITO-Energyville, Belgium

^c Department of Information and Electrical Engineering, Hamburg University of Applied Sciences, Germany

^d Systems Control and Optimization Laboratory, Department of Microsystems Engineering and Department of Mathematics, University of Freiburg, Germany

ARTICLE INFO

Keywords:

Tracking NMPC
Optimal trajectory generation
Airborne wind energy
Warping theory

ABSTRACT

Fast online generation of feasible and optimal reference trajectories is crucial in tracking model predictive control, especially for stability and optimality in presence of a time varying parameter. In this paper, in order to circumvent the operational efforts of handling a discrete set of precomputed trajectories and switching between them, time warping of a single trajectory is proposed as an alternative concept. In particular, the conceptual ideas of *warping theory* are presented and illustrated based on the example of a tethered kite system for airborne wind energy. In detail, for warpable systems, feasibility and optimality of trajectories are discussed. Subsequently, the full algorithm of a nonlinear model predictive control implementation based on warping a single precomputed reference is presented. Finally, the warping algorithm is applied to the airborne wind energy system. Simulation results in presence of real world perturbations are evaluated and compared.

1. Introduction

In most industrial advanced control processes, the plant economic optimization is typically divided into two levels: a first level where the plant optimal steady-state operational point is computed and a second level that receives the operational point and regulates the plant (Rawlings & Amrit, 2009). One choice to implement the second level is *nonlinear model predictive control (NMPC)* (Rawlings & Amrit, 2009), a control scheme that uses the plant model to track the operational setpoints. A variant of this algorithm is a scheme that, instead of computing and tracking a steady-state setpoint, considers a time-varying optimal trajectory. In this scenario, if the second level uses NMPC to track the optimized trajectory, the resultant control scheme is referred to as *tracking NMPC* (Alexis, Nikolakopoulos, & Tzes, 2014; Zanon, Gros, & Diehl, 2016).

While stability theory for tracking NMPC has been developed (Grüne & Pannek, 2011; Rawlings & Amrit, 2009) and despite the algorithm being successfully implemented and demonstrated in different scenarios (Chauhdry & Luh, 2012; Cortinovis, Mercangöz, Mathur, Poland, & Blaumann, 2013; Dutta et al., 2014; Guerreiro, Silvestre, Cunha, & Pascoal, 2014; Nagy, Mahn, Franke, & Allgöwer, 2007; Wiese, Blom, Manzie, Brear, & Kitchener, 2015), it suffers from various issues. In particular, if the trajectories are computed offline, the controller

lacks online adaptation to real disturbances and model mismatches. Moreover, even if the tracking trajectories are recomputed online, the time required to compute a new optimal trajectory introduces delays between the first and the second level (Rawlings & Amrit, 2009); if the system has fast dynamics, these delays prevent the first level to react in time to environmental changes. In both scenarios, if the environmental conditions change, the precomputed trajectory might no longer be optimal nor even feasible.

A possible solution to address the mentioned problems is *economic NMPC*, a type of NMPC that, instead of using a cost function that penalizes the deviation from a tracking trajectory, uses a more general cost function. More specifically, by directly optimizing the quantity that indicates when a trajectory is optimal, economic NMPC has the potential to generate online and track optimal trajectories. In practice, however, ensuring stability for economic NMPC is harder than for tracking NMPC, and as a result, the latter is usually a safer and more stable choice whenever it comes to highly nonlinear and real applications.

A field where the described problems are especially relevant is *airborne wind energy (AWE)* (Ahrens, Diehl, & Schmehl, 2013), a novel type of renewable energy that harvests energy from the wind using flying kites or planes. In particular, the energy extracted by an AWE system is dependent on its flight trajectory, which in turn

* Corresponding author at: Delft Center for Systems and Control, Delft University of Technology, The Netherlands.
E-mail addresses: j.lagogarica@tudelft.nl, jesus.lagogarica@vito.be (J. Lago).

depends on the wind velocity and direction. As these two atmospheric properties might greatly vary in the matter of seconds, any controller that aims at optimally flying an AWE system needs to perform online generation of flying trajectories. Considering the models proposed for AWE systems (Erhard, Horn, & Diehl, 2017; Erhard & Strauch, 2013b; Fagiano, Milanese, & Piga, 2012; Gros, Zanon, & Diehl, 2013), they typically consist of a state space with 4–15 states and highly nonlinear dynamics. As a result, to obtain optimal trajectories, complex nonlinear optimization problems need to be solved (Erhard et al., 2017; Gros et al., 2013), which not only require long computation times, but can even lead to failures of the optimization solvers (Gros et al., 2013). In this scenario, both economic and tracking NMPC have big disadvantages, i.e. the former is less stable and the latter only tracks a suboptimal trajectory computed offline.

In this paper, to address the mentioned problems, an algorithm that tries to merge the benefits of economic and tracking NMPC is proposed. In particular, warping NMPC is presented, a control algorithm for tracking a trajectory that is updated online to ensure that it remains optimal.

The algorithm is based on warping theory, a framework first presented in Lago, Erhard, and Diehl (2017) that is based on two key concepts: warvable systems and warvable optimal control problems. While the theoretical foundations of the algorithm have been presented in Lago et al. (2017), in this paper the algorithm is extended for its implementation in a real system via three contributions:

1. Extension of the warping NMPC concept defined in Lago et al. (2017) into a full algorithm that can be applied in a real system.
2. Application of the algorithm to the simulation of a real system, i.e. an AWE system, showing how the control algorithm can, under real life conditions, track optimal trajectories that change in time.
3. Explanation of the conceptual idea of warping theory. In particular, in Lago et al. (2017), the warping theoretical concepts were defined. In this paper, the intuition behind the theoretical concepts is provided and these concepts are illustrated with explanations based on a real application.

The paper is organized as follows: Section 2 introduces the two main areas related to this research: AWE and NMPC. Section 3 summarizes the warping theory proposed in Lago et al. (2017) and extends it by adding conceptual explanations and examples. Subsequently, Section 4 presents the proposed control algorithm that can be used to generate and control optimal trajectories: warping NMPC. Finally, Section 5 presents the performance of warping NMPC with a real life example: the AWE kite system of the company Skysails.

For notational simplicity, concatenations of several vectors, e.g. $[\mathbf{x}^T, \mathbf{u}^T]^T$, will be shortened as (\mathbf{x}, \mathbf{u}) . Likewise, the concatenation of state \mathbf{x} and control \mathbf{u} vectors will be denoted by \mathbf{y} , i.e. $\mathbf{y} = (\mathbf{x}, \mathbf{u})$.

2. Preliminaries

In this section a brief overview of the theory that is used and modified in this paper is provided.

2.1. Airborne wind energy

AWE is a novel type of renewable energy source that aims at harvesting wind power without incurring the large material costs of traditional wind turbines. In particular, in a standard wind turbine, the bulk of the power is generated by the outer 30% of the rotor blades and the rest of the construction is just needed to keep these wings in their fast crosswind motion (Ahrens et al., 2013). In addition, while the extracted power scales with the square of the height, the mass scales cubically. As a result, the maximum size of standard wind turbines is limited, and thus, they are not capable of reaching and harvesting the significantly higher wind energy potential at higher altitudes (Ahrens et al., 2013).

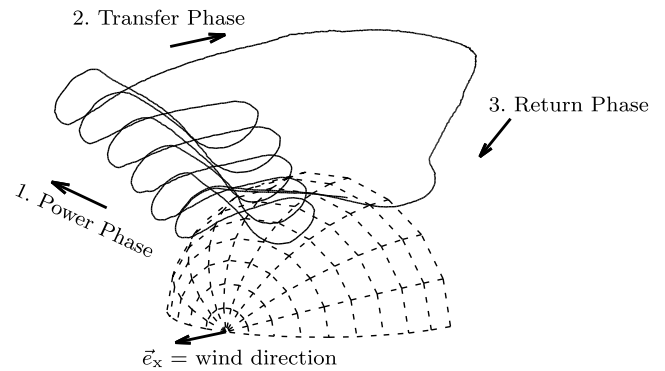


Fig. 1. AWE system pumping cycle: a power phase where the airfoil flies in crosswind motion to produce energy using the high tether forces, a transfer phase to fly to a neutral wind window position, and a return phase to restart the cycle consuming only a fraction of the generated energy (Erhard et al., 2017).

2.1.1. Operational pumping cycle

AWE tries to reduce this problem by redesigning the turbine: it implements the rotor blades as tethered airfoils that are anchored to the ground and fly in crosswind motion. By doing so, it saves significant material costs, and improves the power efficiency as the airfoils can reach higher altitudes where wind speed is stronger and more consistent. To harvest the wind energy, an AWE system can use two working principles: drag or lift mode (Loyd, 1980). In the case of the latter, AWE uses the fact that the lift force on an airfoil increases with the square of the apparent airspeed, i.e., a kite flying in crosswind direction with a velocity five times faster than the wind speed will produce a force on the tethered line 25 times higher than a static kite, to produce high tether forces that rotate a winch with an electric generator at ground level. The operation is done following a periodic cycle where the airfoil unrolls the tether to produce energy and then rolls it back to restart the process. This periodic cycle, usually known as pumping cycle, is illustrated in Fig. 1 and consists of three phases:

1. Power generation phase: the airfoil flies in crosswind motion inducing high line forces to reel out the tether and produce energy on the ground generator.
2. Transfer phase: the airfoil flies to a neutral wind position with low line forces.
3. Return phase: the tether is reeled in and the kite is kept at a neutral wind position so that only a fraction of the generated energy is consumed in this phase.

2.1.2. Dynamical model

In this paper, as a case study, the model for the real AWE system of the Skysails company is considered. This system, which is depicted in Fig. 2, is based on a flying kite.

A model of the system was developed and validated in Erhard and Strauch (2013a) and Erhard and Strauch (2013b). The model is characterized by four states $[\psi, \varphi, \vartheta, l]^T$, two control inputs $[\delta, v_{\text{reel}}]^T$, and two parameters g_k and E . In this definition, l is the tether length, ψ , φ , and ϑ the angles defining the kite position and orientation, δ the kite steering command, and v_{reel} the reeling tether velocity. Based on these definitions, the equations of motion (EOM) are described as:

$$\dot{\psi} = g_k v_a \delta + \dot{\varphi} \cos \vartheta, \quad (1a)$$

$$\dot{\varphi} = -\frac{v_a}{l \sin \vartheta} \sin \psi, \quad (1b)$$

$$\dot{\vartheta} = -\frac{v_w}{l} \sin \vartheta + \frac{v_a}{l} \cos \psi, \quad (1c)$$

$$\dot{l} = v_{\text{reel}}, \quad (1d)$$

with :

$$v_a = v_w E \cos \vartheta - \dot{l} E. \quad (1e)$$

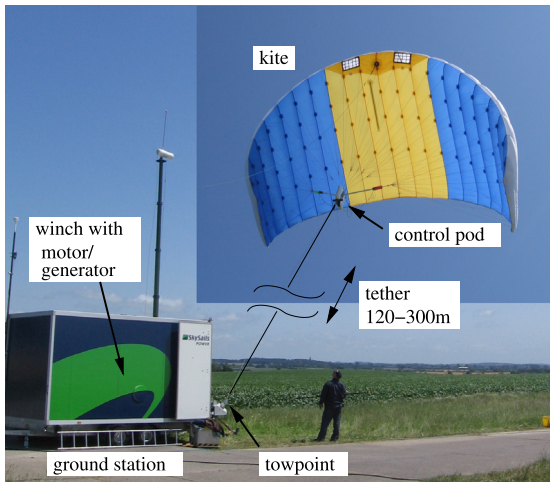


Fig. 2. SkySails kite prototype for power generation in a real flight test (Erhard et al., 2017).

where v_w is the wind ambient velocity and v_a is the air path velocity, i.e., the apparent wind velocity at the kite.

2.1.3. Maximizing extracted energy

Considering the described working principle, the airfoil trajectories should be such that the generated energy in the overall pumping cycle is maximized. However, as the force in the tether and the generated power depends on the wind speed, the trajectory that maximizes the energy varies in time. As a result, to maximize the extracted energy, the airfoil controller needs to generate online optimal trajectories and track them.

In our case study, the importance of maximizing the extracted energy can be easily exemplified. As defined by Erhard et al. (2017), the optimal periodic trajectories $\mathbf{y}^*(t) = (\mathbf{x}^*(t), \mathbf{u}^*(t))$ that maximize the average power in a pumping cycle are obtained by solving the following optimal control problem (OCP):

$$\underset{\mathbf{y}(\cdot), T}{\text{minimize}} \quad J = -\frac{1}{T} \int_0^T v_a(t)^2 \dot{t}(t) dt \quad (2a)$$

$$\text{subject to } \Phi(\mathbf{x}(t), \mathbf{u}(t), v_w) = \dot{\mathbf{x}}(t), \quad t \in [0, T] \quad (2b)$$

$$\mathbf{h}(\mathbf{x}(t), \delta(t)) \leq 0, \quad t \in [0, T] \quad (2c)$$

$$v_{\min} \leq v_{\text{reel}}(t) \leq v_{\max}, \quad t \in [0, T] \quad (2d)$$

$$\mathbf{x}(0) - \mathbf{x}(T) = 0. \quad (2e)$$

In the OCP above, as tether force scales with the square of v_a , $v_a(t)^2 \dot{t}(t)$ in (2a) represents a quantity proportional to the mechanical power. Furthermore, representing the limits on the controls, the constraints of the real system are ensured by (2c)–(2d). Finally, periodicity of the optimal trajectories is guaranteed by (2e).

If this OCP is solved and the average extracted power in a pumping cycle is computed, the power efficiency of the optimal trajectories can be in turn compared with the trajectories of the current controller. In particular, the optimal trajectories have an efficiency of 35% of the so called Loyd limit (Loyd, 1980), which is almost double the 18% efficiency obtained by the previously proposed controller (Erhard & Strauch, 2015), i.e., optimal trajectories can extract a double amount of energy in comparison with the current controller.

Note that, in the context of AWE, efficiency is defined as the ratio between the extracted average power in a pumping cycle divided by the maximum ideal power as defined by Loyd (Loyd, 1980):

$$\eta_{\text{Loyd}} = \frac{J}{\frac{4}{27} E^2 v_w^3}, \quad (3)$$

where J is defined by (2a) and the nominator is adjusted accordingly to the AWE model (Erhard et al., 2017).

2.2. Nonlinear model predictive control

Nonlinear model predictive control (NMPC) is a family of predictive control algorithms that, by means of a dynamical model, try to anticipate the future and to select the optimal control policy that optimizes a given cost function. Its basic working principle is to solve an OCP at each time iteration to obtain an optimal control trajectory \mathbf{U}^* that ensures the system dynamics as well as other constraints. In particular, the controller strategy can be described as follows:

1. First, the controller receives information regarding the current system state $\bar{\mathbf{x}}_0$.
2. Then, it solves an OCP in order to obtain the optimal control trajectory \mathbf{U}^* . In this scenario the decision variables are the controls $\mathbf{U} = (\mathbf{u}_0, \mathbf{u}_1, \dots, \mathbf{u}_{N-1})$ and the states $\mathbf{X} = (\mathbf{x}_0, \mathbf{x}_1, \dots, \mathbf{x}_N)$.
3. Once the OCP is solved, the algorithm applies the first optimal control \mathbf{u}_0^* to the system, it moves the optimization horizon a time step forward, observes the new state $\bar{\mathbf{x}}_0$, and repeats the procedure from 1.

In the case of tracking NMPC, the cost function minimizes the least squares error between the predicted trajectories \mathbf{X} and \mathbf{U} and some reference trajectories \mathbf{X}_r and \mathbf{U}_r , which are usually obtained by means of an offline OCP. In detail, tracking NMPC solves at every iteration the following problem:

$$\min_{\mathbf{X}, \mathbf{U}} \sum_{k=0}^{N-1} \left(\|\mathbf{x}_{r,k} - \mathbf{x}_k\|_{\mathbf{Q}}^2 + \|\mathbf{u}_{r,k} - \mathbf{u}_k\|_{\mathbf{R}}^2 \right) + E(\mathbf{x}_N) \quad (4a)$$

$$\text{s.t. } \mathbf{x}_0 - \bar{\mathbf{x}}_0 = 0 \quad (4b)$$

$$\Phi_k(\mathbf{x}_k, \mathbf{u}_k) - \mathbf{x}_{k+1} = 0, \quad k = 0, \dots, N-1 \quad (4c)$$

$$\mathbf{h}(\mathbf{x}_k, \mathbf{u}_k) \leq 0, \quad k = 0, \dots, N-1 \quad (4d)$$

$$\mathbf{r}(\mathbf{x}_N) \leq 0, \quad (4e)$$

with matrices $\mathbf{Q} > 0$ and $\mathbf{R} > 0$, $\mathbf{X}_r = (\mathbf{x}_{r,0}, \dots, \mathbf{x}_{r,N})$ and $\mathbf{U}_r = (\mathbf{u}_{r,0}, \dots, \mathbf{u}_{r,N-1})$, and the equation for the system dynamics $\mathbf{x}_{k+1} = \Phi_k(\mathbf{x}_k, \mathbf{u}_k)$.

2.3. Numerical optimization

In order to solve the OCPs and NMPC problems defined in this paper, the Casadi (Andersson, 2013) framework for dynamic optimization and the optimization solver IPOPT (Wächter & Biegler, 2006) are employed.

In addition, to discretize the dynamics of the AWE system, a direct method is used: multiple shooting (Bock & Plitt, 1984); further details on how to implement this method for the considered AWE system are given in Erhard et al. (2017) and Lago Garcia (2016).

3. Warping: Theory and application

In this section, the definition of the concepts that warping NMPC is based on are provided: warpage systems and warpage optimal control problems. In order to exemplify these concepts and provide the intuition behind them, the flying trajectories of the AWE system are employed. A more formal definition of warping theory is elaborated in the appendices and in Lago et al. (2017).

3.1. Empirical observation in optimal solutions

For the considered AWE system, if its optimal trajectories are regarded as a function of the wind speed, a very interesting phenomenon

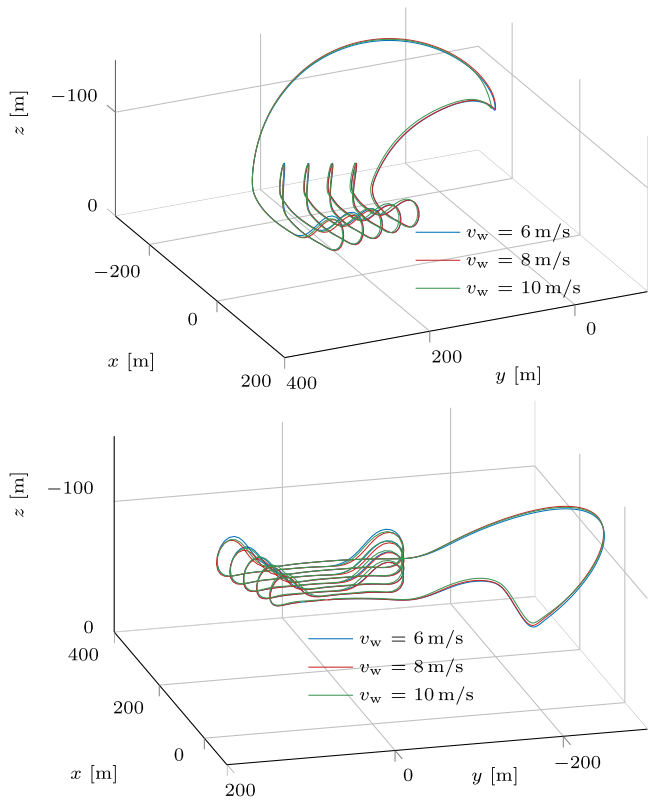


Fig. 3. 3D views of the optimal trajectories obtained by solving the OCP (2a)–(2e) for different v_w values.

can be observed: as depicted in Fig. 3, the periodic optimal trajectories at different wind speeds represent the same 3D flight paths.

However, when these trajectories are regarded in the time domain, it can be observed how, while all optimal trajectories make the kite fly through the same physical locations, the velocity of the kite at each trajectory is different.

However, when these trajectories are regarded in the time domain, it can be observed how, while all optimal trajectories make the kite fly through the same physical locations, the velocity of the kite at each trajectory is different. More specifically, while the trajectories are the same, the time it takes for the kite to fly them is dependent on the wind velocity. This effect can be further explained looking at Fig. 4, which illustrates the periodic optimal trajectories of two of the states for different wind speeds and in different time frames.

Indeed, if we consider the 2D optimal trajectories at $v_w = 10$ m/s, $v_w = 8$ m/s, and $v_w = 6$ m/s, we can easily show that, defining each trajectory in a different time frame, the 3 trajectories represent the same 2D path. This concept is perfectly depicted in Fig. 4: defining the optimal trajectory for $v_w = 10$ m/s in a time frame τ_{10} , and the optimal trajectories for $v_w = 8$ m/s and $v_w = 6$ m/s in the warped time frames $\tau_8 = \frac{10}{8}\tau_{10}$ and $\tau_6 = \frac{10}{6}\tau_{10}$, it can be observed that the three trajectories are exactly the same. In other words, warping in time the trajectories at $v_w = 8$ m/s and $v_w = 6$ m/s with ratios $\frac{10}{8}$ and $\frac{10}{6}$ leads to the same optimal trajectory obtained for $v_w = 10$ m/s.

This same phenomenon, as shown in Fig. 5, can also be noticed in the inputs of the system.

3.2. Conceptual idea of warping

As these trajectories are the same in the 3D space but different in the time domain, they can be interpreted as time warped versions of each other. In particular, an optimal trajectory for a certain wind speed

could be obtained by squeezing or extending. i.e., warping in time, the optimal trajectory at any other given wind speed.

This concept of translating between optimal trajectories at different wind speeds is defined as warping. Similarly, any dynamic system with the necessary properties to implement warping will be denoted as a warpable system. Both concepts, i.e. warping and warpable systems, will be the key concepts of the control algorithm that is proposed. In the following sections, the two concepts are formalized and the intuition behind them is provided.

3.3. Warpable dynamical system

A warpable dynamical system (WDS) is any dynamical system whose dynamics have the following structure:

$$\begin{aligned} \dot{\mathbf{x}}(t) &= p(t)\mathbf{f}(\mathbf{x}(t), \mathbf{u}_1(t)) + \mathbf{L}(\mathbf{x}(t), \mathbf{u}_1(t))\mathbf{u}_2(t) \\ &= p(t)\mathbf{g}(t) + \mathbf{S}(t)\mathbf{u}_2(t), \end{aligned} \quad (5)$$

where $\mathbf{x} \in \mathbb{R}^m$ is the system state, $\mathbf{u}_1 \in \mathbb{R}^{n_1}$ and $\mathbf{u}_2 \in \mathbb{R}^{n_2}$ the system inputs, and $p \in \mathbb{R}$ a time dependent positive parameter. Note that $p(t)$ is assumed to be positive without loss of generality as the sign of $p(t)$ could be transferred to $\mathbf{g}(t)$ and $\mathbf{f}(\cdot)$.

Recalling now the EOM of the AWE kite system, i.e. (1a)–(1e), it is easy to show that it is a WDS system. In particular, substituting Eq. (1e) into Eqs. (1a), (1b) and (1c), (1b) into (1a), and (1d) into (1e), yields the following equivalent EOM:

$$\dot{\psi} = v_w \left(\cos \vartheta E g_k \delta - \frac{E \sin \psi}{l \tan \vartheta} \cos \vartheta \right) + v_{\text{reel}} \left(\frac{E}{l \tan \vartheta} - E g_k \delta \right) \quad (6a)$$

$$\dot{\varphi} = v_w \frac{-E \sin \psi}{l \tan \vartheta} + v_{\text{reel}} \frac{E}{l \sin \vartheta}, \quad (6b)$$

$$\dot{\vartheta} = v_w \left(-\frac{\sin \vartheta}{l} + \frac{E \cos \vartheta \cos \psi}{l} \right) - v_{\text{reel}} \frac{E \cos \psi}{l}, \quad (6c)$$

$$\dot{l} = v_{\text{reel}}. \quad (6d)$$

Therefore, the kite is a WDS with $\mathbf{u}_1 = [\delta]$, $\mathbf{u}_2 = [v_{\text{reel}}]$, and $p = v_w$.

This type of dynamical systems is interesting because of its warping property w.r.t. the parameter p : any feasible trajectory for a parameter value $p = p_1$ can be warped in time to obtain a feasible trajectory for any other parameter value $p = p_2$. More specifically, this property allows to compute a feasible solution for the general system (5), given a feasible trajectory $(\mathbf{x}_{\text{ref}}(\tau), \mathbf{u}_{1,\text{ref}}(\tau), \mathbf{u}_{2,\text{ref}}(\tau))$ for a reference WDS system. In particular, a feasible trajectory of (5) is given by:

$$\mathbf{x}(t) = \mathbf{x}_{\text{ref}}(w(t)), \quad (7a)$$

$$\mathbf{u}_1(t) = \mathbf{u}_{1,\text{ref}}(w(t)), \quad (7b)$$

$$\mathbf{u}_2(t) = \dot{w}(t)\mathbf{u}_{2,\text{ref}}(w(t)), \quad (7c)$$

where $w(t)$ is called warping factor and is defined by:

$$\dot{w}(t) = \frac{d\tau}{dt} = \frac{p(t)}{p_{\text{ref}}} \quad (8)$$

Formally, this property is defined by Lemma A.1 in Appendix A. The interpretation behind the lemma is simple: all feasible trajectories of WDS are equal to each other but defined in different time frames. The relation between any of these trajectories is simply computed by the warping factor $w(t)$, which represents the relation between the velocities of the dynamics dt and $d\tau$ in the different frames. The exception to that rule is the \mathbf{u}_2 subset of inputs, which not only is warped in time, but also amplified or attenuated to account for the $p(t)$ -independence of the second term of Eq. (5). Note that (7c) can be given as $\mathbf{u}_2(t) = \mathbf{u}_{2,\text{ref}}(\tau)p(t)/p_{\text{ref}}$.

In the AWE system, the wind velocity v_w is the warping parameter, and thus, it determines the speed of the system dynamics and the relation between feasible trajectories. This effect, formalized by the EOM and Lemma above, is actually what was shown in Figs. 4 and 5, where trajectories at different wind speeds had the same 3D trajectory at different time scales.

In this example, note the effect that warping has on the control v_{reel} , which, as defined by (7c), not only is warped but also attenuated or amplified. This transformation can be observed in Fig. 6, which extends the warping scenario of Figs. 4–5 to the control v_{reel} .

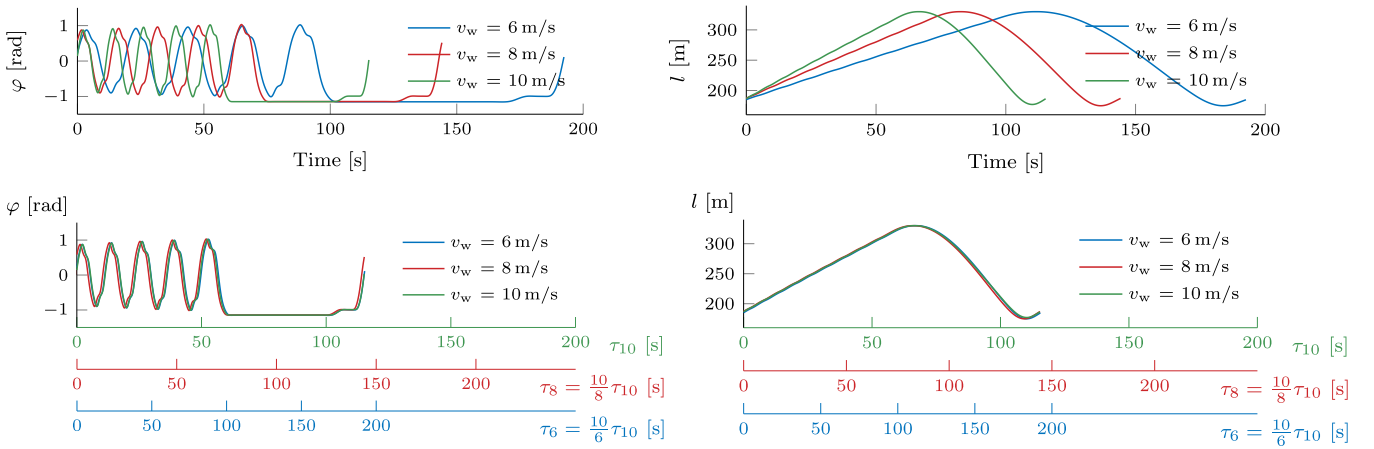


Fig. 4. Top: Optimal states φ and l for different v_w values. Bottom: optimal states φ and l for different v_w values but defined at three different time frames. The optimal trajectory for $v_w = z$ m/s is defined in the time frame τ_z . It can be observed how the optimal trajectories are time warped versions of each other.

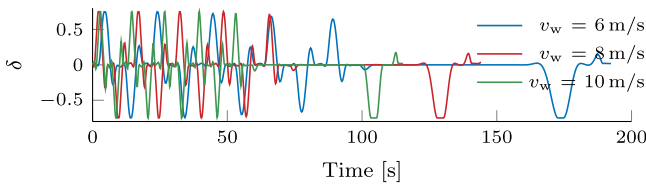


Fig. 5. Optimal input δ for different v_w values (Lago et al., 2017).

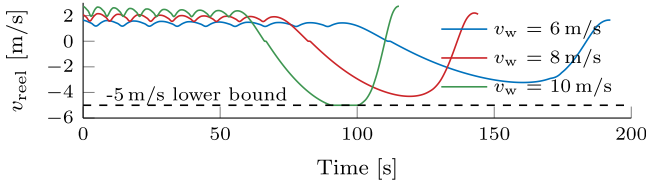


Fig. 6. Optimal input control v_{reel} for different v_w values (Lago et al., 2017).

3.4. Preservation of optimality in warping

As it will be explained in Section 4, the basic idea of the proposed controller is to compute one reference trajectory for a reference parameter p_{ref} , and apply the warping transformation to adapt the tracking trajectory to the time varying parameter $p(t)$. As a result, when warping trajectories, not only feasibility is important but also maintaining optimality is highly desirable.

3.4.1. Warpable optimal control problems

In the context of warping, it can be shown that optimality is maintained if the warped trajectory is the solution of a *Warpable Optimal Control Problem (WOCP)*:

$$\begin{aligned} \text{WOCP}(p) : & \\ \min_{\mathbf{y}(\cdot), T} \int_0^T L_1(p) L_2 \left(\mathbf{x}(t), \mathbf{u}_1(t), \frac{\mathbf{u}_2(t)}{p} \right) dt & \quad (9a) \\ \text{s.t. } p \mathbf{g}(t) + \mathbf{S}(t) \mathbf{u}_2(t) = \dot{\mathbf{x}}(t), \quad t \in [0, T] & \quad (9b) \\ \mathbf{h}(\mathbf{x}(t), \mathbf{u}_1(t)) \leq 0, \quad t \in [0, T] & \quad (9c) \\ \mathbf{r}(\mathbf{x}(0), \mathbf{x}(T)) \leq 0. & \quad (9d) \end{aligned}$$

In this case, due to the absence of \mathbf{u}_2 constraints and the structure of the objective function, optimal solutions $\mathbf{y}^*(t)$ for any parameter p can be obtained by warping an optimal solution $\mathbf{y}_{ref}^*(t)$ computed for a reference

parameter p_{ref} . This very interesting property is formally defined by [Theorem B.1](#) in [Appendix B](#).

3.4.2. Semi-warpable optimal control problems

While the solutions of WOCPs preserve optimality, the WOCP structure has a big limitation: \mathbf{u}_2 cannot be constrained. In terms of the AWE system, this implies that the optimal trajectories cannot bound the reeling speed $[v_{reel}] = \mathbf{u}_2$; that is obviously not possible as the trajectories have to ensure that v_{reel} remains within the safety bounds.

This problem can be better understood regarding [Fig. 6](#) displaying the optimal trajectories at different wind speeds: if the trajectory at $p_{ref} = 6$ m/s is taken as a reference, the warping transformation for $p = 8$ m/s would generate the shown graph for 8 m/s. Indeed, as the optimal trajectory at 8 m/s does not reach the bounds for v_{reel} , the warped trajectory is exactly equal to the optimal one. However, the same does not hold for the trajectory at $p = 10$ m/s; particularly, as observed from [Fig. 6](#), the optimal trajectory at $p = 10$ m/s reaches the -5 m/s bound of v_{reel} . Therefore, in this case, if the trajectory at $p_{ref} = 6$ m/s is warped, the warped trajectory would contain v_{reel} values that would violate the \mathbf{u}_2 constraint $v_{reel} \geq -5$ m/s (note that the control v_{reel} is limited at -5 m/s).

Semi-Warpable Optimal Control Problem (SWOCP) is a class of OCPs that solve this issue by generalizing the WOCP structure to the case of having \mathbf{u}_2 path constraints:

$$\begin{aligned} \text{SWOCP}(p) : & \\ \text{WOCP}(p) & \quad (10a-10d) \\ \mathbf{h}_2(\mathbf{x}(t), \mathbf{u}_1(t), \mathbf{u}_2(t)) \leq 0 \quad t \in [0, T] & \quad (10e) \end{aligned}$$

For a more detailed and formal definition of SWOCPs we refer to [Appendix B.2](#).

The key distinction w.r.t. to an WOCP is that, by adding the \mathbf{u}_2 -dependent constraints, warped trajectories might no longer satisfy the path constraints of the OCP:

$$\begin{aligned} \mathbf{h}_2(\mathbf{x}_{ref}^*(\tau), \mathbf{u}_{1,ref}^*(\tau), \mathbf{u}_{2,ref}^*(\tau)) \leq 0 & \\ \implies \mathbf{h}_2(\mathbf{x}_p(t), \mathbf{u}_{p1}(t), \frac{p_{ref}}{p} \mathbf{u}_{p2}(t)) \leq 0 & \\ \not\Rightarrow \mathbf{h}_2(\mathbf{x}_p(t), \mathbf{u}_{p1}(t), \mathbf{u}_{p2}(t)) \leq 0. & \quad (11) \end{aligned}$$

Based on the observation above, the natural question that arises is then: if warping might violate the path constraint, how can warping preserve optimality for SWOCP-generated trajectories? The answer to that question are best warpable references.

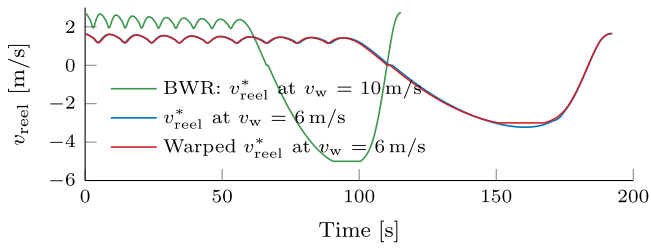


Fig. 7. Comparison between optimal v_{reel} and suboptimal v_{reel} computed from a BWR (Note that $v_{w,max} = 10$ m/s is assumed in this case).

3.4.3. Best warpable references

Given the optimal solution $\mathbf{y}_{bwr}^*(t)$ of a SWOCP(p_{bwr}), i.e. a SWOCP defined for a reference parameter p_{bwr} , $\mathbf{y}_{bwr}^*(t)$ is defined to be a *best warpable reference (BWR)* if all the warped trajectory of $\mathbf{y}_{bwr}^*(t)$ satisfy the \mathbf{u}_2 -dependent constraints of the SWOCP.

A very interesting property of BWRs is that, provided that a BWR exist for a given SWOCP and that the \mathbf{u}_2 -dependent constraints are inactive at the BWR, the BWR can be regarded as an optimal reference trajectory. More specifically, any warped trajectory $\mathbf{y}_p(t)$, obtained by warping the optimal solution $\mathbf{y}_{ref}^*(\tau)$ of the reference SWOCP(p_{ref}) = SWOCP(p_{bwr}), is also an optimal solution of the general SWOCP(p).

This interesting property is formally defined in Corollary B.1 of Appendix B. Similarly, BWRs are formally defined in Definition B.2 of the same appendix.

When considering this property, it is also necessary to analyze the implications of having \mathbf{u}_2 -dependent constraints that are active at the BWR. In particular, if \mathbf{h}_2 is active for p_{bwr} , i.e. $\mathbf{h}_2(\mathbf{y}_{bwr}(\tau)) = 0$, the warped trajectories $\mathbf{y}_p(t)$ are usually suboptimal. In this case, since they are still feasible and are generated from an optimal trajectory, they still represent a better solution than a random feasible trajectory. This issue is illustrated in Fig. 7, where a warped trajectory obtained from the BWR is compared to the optimal trajectory v_{reel}^* at $v_w = 6$ m/s.

For the proposed algorithm, the above property has a very important implication: if computation of a BWR is possible, the BWR can be used as a reference trajectory to generate optimal or suboptimal trajectories for any parameter p . As shown in Theorem B.2 of Appendix B, there are some ways to compute BWRs. For our case study, it is only important to know the following one: if the path-constraint $\mathbf{h}_2(\mathbf{x}(t), \mathbf{u}_1(t), \mathbf{u}_2(t))$ can be reformulated as:

$$\mathbf{f}_{lower}(\mathbf{x}(t), \mathbf{u}_1(t)) \leq \mathbf{u}_2(t) \leq \mathbf{f}_{upper}(\mathbf{x}(t), \mathbf{u}_1(t)), \quad (12)$$

where : $\mathbf{f}_{lower}(\mathbf{x}, \mathbf{u}_1) \leq 0, \quad \mathbf{f}_{upper}(\mathbf{x}, \mathbf{u}_1) \geq 0.$

the solution of SWOCP(p_{max}), i.e. the SWOCP version where the parameter p is at its maximum value, is a BWR. A formal proof of this property is given by Theorem B.2 in Appendix B.

3.4.4. Optimality of AWE trajectories

Using the above properties and definitions, it can be shown that optimality is preserved when warping the trajectories of the AWE system. In particular, recalling (2) as the OCP that optimized the flying trajectories, (1e) can be used to expand the cost function as:

$$\begin{aligned} J &= -\frac{1}{T} \int_0^T v_a^2 dt = -\frac{1}{T} \int_0^T (v_w E \cos \vartheta - v_{reel} E)^2 v_{reel} dt \\ &= -\frac{v_w^3}{T} \int_0^T \left(E \cos \vartheta - \left(\frac{v_{reel}}{v_w} \right) \right)^2 \left(\frac{v_{reel}}{v_w} \right) dt \end{aligned} \quad (13)$$

Considering this reformulation and (2a)–(2e), it is clear that the flying trajectories are solutions of a SWOCP. Then, since (2d) has the structure of (12), a BWR is given by the OCP solution at the maximum wind speed v_w .

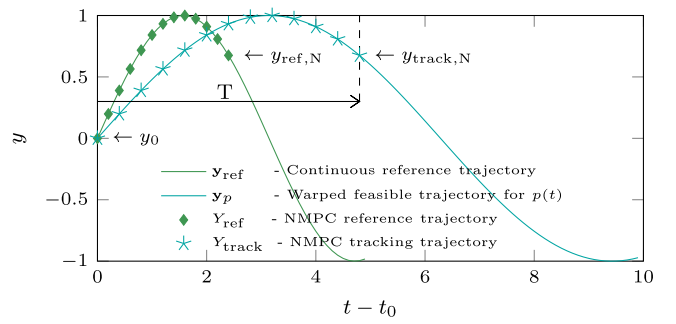


Fig. 8. Warping NMPC example with $\dot{w}(t) = \frac{p(t)}{p_{ref}} = \frac{1}{2}$ and $\mathbf{y} = [y] \in \mathbb{R}^1$.

4. Warping NMPC

Once the theoretical foundations of warping are defined, *warping NMPC* can be finally introduced. Within the algorithm, two different control applications will be distinguished: tracking of general feasible trajectories and tracking of optimal trajectories.

4.1. Generation of feasible trajectories

In its first variant, warping NMPC uses a feasible trajectory for a reference parameter p_{ref} as a reference trajectory $\mathbf{y}_{ref}(\tau)$. In particular, at each iteration, it reads from the environment the $p(t)$ value. Based on it, it warps $\mathbf{y}_{ref}(\tau)$ to obtain a feasible trajectory $\mathbf{y}_p(t)$ for the $p(t)$ value. Finally, it updates the tracking trajectory with $\mathbf{y}_p(t)$.

Fig. 8 illustrates this concept: \mathbf{y}_{ref} , feasible for a constant p_{ref} , is computed offline. Then, by time warping \mathbf{y}_{ref} online, warping NMPC generates a feasible tracking trajectory for the real $p(t)$. In a computer implementation, a discrete precomputed reference trajectory $\mathbf{Y}_{ref} = (\mathbf{y}_{ref,0}, \dots, \mathbf{y}_{ref,N})$ is used to obtain the discrete tracking trajectory at the current time $\mathbf{Y}_{track} = (\mathbf{y}_{track,0}, \dots, \mathbf{y}_{track,N})$.

4.2. Generation of optimal trajectories

In a second and third variants, warping NMPC extends the case of tracking feasible trajectories to tracking optimal trajectories. In particular, to ensure that tracking trajectories are optimal, the new NMPC scheme follows the procedure described for feasible trajectories, but computing the reference trajectory $\mathbf{y}_{ref}(\tau)$ in a very distinct manner. In particular, to obtain $\mathbf{y}_{ref}(\tau)$, it considers one of two possibilities:

1. Computing $\mathbf{y}_{ref}(\tau)$ as the solution of a WOCPP(p), i.e. $\mathbf{y}_{ref}(\tau) = \mathbf{y}_{ref}^*(\tau)$. In that case, due to the property of WOCPPs, any tracking trajectory $\mathbf{y}_p(t)$ obtained from warping $\mathbf{y}_{ref}^*(\tau)$ will also be optimal.
2. Computing $\mathbf{y}_{ref}(\tau)$ as the BWR of a SWOCP(p), i.e. $p_{ref} = p_{bwr}$. In this case, as explained in Section 3.4.3, the warped tracking trajectories $\mathbf{y}_p(t)$ will be either optimal or suboptimal depending on whether $\mathbf{h}_2(\cdot)$ is inactive or active at $\mathbf{y}_{ref}(\tau)$.

4.3. Algorithm

Whether the algorithm uses the variant defined in Section 4.1 or one of the two variants defined in Section 4.2, its implementation is the same. In particular, in a computer implementation, warping NMPC uses the same scheme as a traditional tracking NMPC, but updates the tracking trajectory \mathbf{Y}_{track} in a different manner.

4.3.1. Traditional shifting

A classical tracking NMPC scheme updates the tracking trajectory \mathbf{Y}_{track} at each iteration by shifting one time step backwards the latest

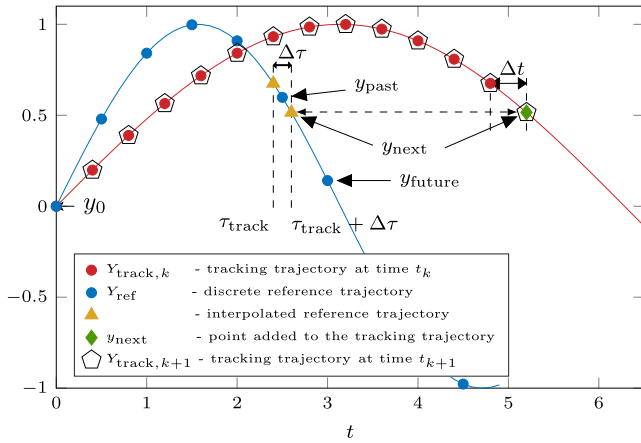


Fig. 9. Warping NMPC shifting strategy for $y = [y] \in \mathbb{R}^1$: τ_{track} is used to follow the last point of $\mathbf{Y}_{\text{track}}$ within the reference trajectory \mathbf{y}_{ref} .

$\mathbf{Y}_{\text{track}}$ and adding a new point \mathbf{y}_{new} at the end of it. To compute \mathbf{y}_{new} , the NMPC regards a fixed reference trajectory $\mathbf{Y}_{\text{ref}} = (\mathbf{y}_{\text{ref},0}, \dots, \mathbf{y}_{\text{ref},M})$ defined in a fixed reference time grid $\mathbf{t}_{\text{ref}} = [t_{\text{ref},0}, \dots, t_{\text{ref},M}]$. Then, defining the Δt in the reference time grid as the Δt of the NMPC, \mathbf{y}_{new} is simply selected from \mathbf{Y}_{ref} . The following equations illustrate the update:

$$\begin{aligned} t_k &: \mathbf{Y}_{\text{track},k} = (\mathbf{y}_{\text{ref},k}, \mathbf{y}_{\text{ref},k+1}, \dots, \mathbf{y}_{\text{ref},k+N}) \\ t_{k+1} &: \mathbf{Y}_{\text{track},k+1} = (\mathbf{y}_{\text{ref},k+1}, \dots, \mathbf{y}_{\text{ref},k+N}, \mathbf{y}_{\text{new}}) \end{aligned} \quad (14)$$

with :

$$\mathbf{y}_{\text{new}} = \mathbf{y}_{\text{ref},k+1+N}$$

This type of update, i.e. just updating the last value of $\mathbf{Y}_{\text{track}}$ and shifting the others, is done to avoid big changes on the optimization problem, and in turn, to improve the stability of the NMPC.

4.3.2. Shifting in warping NMPC

In order to preserve this stability property in the proposed warping NMPC, $\mathbf{Y}_{\text{track}}$ is also updated with this shifting scheme. However, instead of using a fixed reference trajectory in a fixed time frame and directly selecting \mathbf{y}_{new} from it, the new scheme uses a reference trajectory $\mathbf{Y}_{\text{ref}} = (\mathbf{y}_{\text{ref},0}, \dots, \mathbf{y}_{\text{ref},M})$ in a reference time grid $\tau_{\text{ref}} = [\tau_{\text{ref},0}, \tau_{\text{ref},1}, \dots, \tau_{\text{ref},M}]$ and selects \mathbf{y}_{new} by finding the relation between τ_{ref} and the real time grid \mathbf{t} . In this context, the real time grid $\mathbf{t} = [t_0, \dots, t_M]$ represents the sampling interval of the real-time operational controller, and τ_{ref} represents a warped version of \mathbf{t} .

Defining the controller sampling time as Δt , the time point at the end of the NMPC horizon by t_N , the equivalent point of t_N in the warped time frame τ_{ref} by τ_N , and considering a NMPC horizon of $N + 1$ points, the algorithm to update \mathbf{y}_{new} consists of five steps:

1. The algorithm reads the new value of p .
2. The algorithm uses a continuous time variable τ_{track} to track τ_N . To do so, τ_{track} is updated at each iteration by increasing its value by a warped time step $\Delta\tau = \Delta t \frac{p}{p_{\text{ref}}}$.
3. As t_N represents the time location of \mathbf{y}_{new} in the real time grid, τ_{track} represents the time location of \mathbf{y}_{new} in the warped time grid τ_{ref} . Therefore, \mathbf{y}_{new} is updated by finding τ_{track} in τ_{ref} , and interpolating \mathbf{Y}_{ref} accordingly.
4. The control \mathbf{u}_2 of \mathbf{y}_{new} is attenuated/amplified in order to fulfill the warping equivalence between \mathbf{Y}_{ref} and $\mathbf{Y}_{\text{track}}$.
5. The new $\mathbf{Y}_{\text{track}}$ is built by shifting the previous $\mathbf{Y}_{\text{track}}$ and adding \mathbf{y}_{new} at the end.

This algorithm is represented in Algorithm 1 and illustrated in Fig. 9. An important fact is that the trajectory adaptability to the changes on $p(t)$ have a delay equal to the NMPC horizon length. However, for many applications, this is rarely a real problem due to the short NMPC horizons.

Algorithm 1 Warping NMPC

```

1: function UPDATETRACKINGTRAJECTORY( $\mathbf{Y}_{\text{track}}$ )
2:   ▷ Update warping parameter  $p$ 
3:    $p \leftarrow \text{readLatestMeasurement}()$ 
4:   ▷ Compute warped time step
5:    $\Delta\tau \leftarrow \Delta t \frac{p}{p_{\text{ref}}}$ 
6:   ▷ Update tracking variable
7:    $\tau_{\text{track}} \leftarrow \tau_{\text{track}} + \Delta\tau$ 
8:   ▷ Generate next tracking point
9:    $\mathbf{y}_{\text{next}} \leftarrow \text{nextTrackingPoint}(\tau_{\text{track}}, p)$ 
10:  ▷ Update tracking trajectory
11:   $\mathbf{Y}_{\text{track}} \leftarrow \text{shiftAndAdd}(\mathbf{Y}_{\text{track}}, \mathbf{y}_{\text{next}})$ 
12:  return  $\mathbf{Y}_{\text{track}}$ 
13: end function
14:
15: function NEXTTRACKINGPOINT( $\tau_{\text{next}}, p$ )
16:  ▷ Compute closest past reference point
17:   $\tau_{\text{past}} \leftarrow \arg \min_{\tau} |\tau - \tau_{\text{next}}|,$ 
18:  s.t.  $\tau \leq \tau_{\text{next}}, \tau \in \tau_{\text{ref}}$ 
19:   $\mathbf{y}_{\text{past}} \leftarrow \mathbf{y}_{\text{ref}}(\tau_{\text{past}}),$ 
20:  ▷ Compute closest future reference point
21:   $\tau_{\text{future}} \leftarrow \arg \min_{\tau} |\tau - \tau_{\text{next}}|,$ 
22:  s.t.  $\tau > \tau_{\text{next}}, \tau \in \tau_{\text{ref}}$ 
23:   $\mathbf{y}_{\text{future}} \leftarrow \mathbf{y}_{\text{ref}}(\tau_{\text{future}})$ 
24:  ▷ Interpolate
25:   $\mathbf{y}_{\text{next}} \leftarrow \mathbf{y}_{\text{past}} + \frac{\mathbf{y}_{\text{future}} - \mathbf{y}_{\text{past}}}{\tau_{\text{future}} - \tau_{\text{past}}} (\tau_{\text{next}} - \tau_{\text{past}})$ 
26:  ▷ Attenuate controls  $\mathbf{u}_2$ 
27:   $\mathbf{y}_{\text{next}}(\mathbf{u}_2) \leftarrow \mathbf{y}_{\text{next}}(\mathbf{u}_2) \frac{p}{p_{\text{ref}}}$ 
28:  return  $\mathbf{y}_{\text{next}}$ 
29: end function

```

4.4. Implementation details

In order to implement the described algorithm, there are two implementation details that have to be taken into account:

4.4.1. Trajectory discretization

While all the mathematical proofs have been given for continuous time trajectories, the implementation of the algorithm is done in discrete time. Particularly, the trajectories employed by the algorithm are obtained by interpolating between the values of the continuous trajectories at a predefined discrete time grid. As a result, the trajectories employed by the algorithm are approximations of the continuous counterparts.

To ensure that the properties of optimality and feasibility of the continuous case are preserved in the discrete case, i.e. to ensure that the discretized trajectory accurately approximates the continuous one, the NMPC algorithm should employ a small enough sampling time Δt . Particularly, the implementation of the algorithm should ensure that $\Delta t \ll \tau_{\text{ref},M}$, with $\tau_{\text{ref},M}$ defining the time duration of the reference trajectory.

The exact relation between Δt and $\tau_{\text{ref},M}$ that guarantees a good approximation will obviously depend on the application. For the case study presented in this paper, i.e. an AWE system, we show that $2000 \Delta t \approx \tau_{\text{ref},M}$ is small enough to ensure that the discrete trajectories accurately approximate the continuous ones. Particularly, as we will show in the next section, considering a sampling time $\Delta t = 100$ ms for a $\tau_{\text{ref},M} \approx 200$ s, the discrete reference trajectory can be warped in time and still ensures feasibility and optimality.

4.4.2. Measuring $p(t)$

The parameter $p(t)$ is arguably the most important parameter in the proposed algorithm. Particularly, as $p(t)$ determines the warping relation, it is paramount to have $p(t)$ measurements updated fast enough so that the warped trajectories that the NMPC tracks stay feasible/optimal.

Table 1
Efficiency comparison of optimal solutions and trajectories obtained by warping.

v_w	6 m/s	8 m/s	10 m/s	12 m/s	14 m/s	15 m/s
η_{Loyd} optimal	35.4%	35.4%	35.3%	34.9%	34.2%	33.7%
η_{Loyd} warping	33.7% (all wind speeds)					

In particular, in order to guarantee that the warped trajectories remain optimal and feasible, the measurement interval of $p(t)$ should be lower than the sampling time Δt of the controller.

5. AWE system control via warping NMPC

The proposed algorithm can now be used to control the AWE system, which needs to track optimal trajectories that change as a function of the wind speed. However, before implementing the algorithm, it needs to be ensured that the system satisfies the requirements of warping NMPC, i.e. that the kite is a WDS and that the system’s optimal trajectories are the solution of a SWOCP.

As defined in Section 3.3, the kite is a warpage system with $\mathbf{u}_1 = [\delta]$, $\mathbf{u}_2 = [v_{reel}]$, and $p = v_w$. In particular, the wind velocity v_w is a warpage parameter that determines the speed of the system dynamics. Moreover, as defined in Section 3.4.4, the optimal trajectories are the solution of a SWOCP. In particular, a BWR can be computed using the maximum v_w -value (15 m/s in our real system). Based on these results, warpage NMPC can indeed be used to perform online generation and tracking of optimal trajectories by using the BWR as the reference trajectory.

5.1. Efficiency of BWR

As a first step before implementing warpage NMPC, the efficiency quality of the considered BWR needs to be evaluated. In particular, since at the optimal solution \mathbf{y}_{ref}^* for $v_w = 15$ m/s the constraint (2d) is active, the warped tracking trajectories are suboptimal (refer to Section 3.4.3 and the remark of Corollary B.1). Therefore, to evaluate the decrease in optimality of when using warped trajectories, Table 1 compares the power efficiency (as given by (3)) of optimal trajectories at different $p = v_w$ values with respect to their warped counterparts.

Considering that explicitly solving the SWOCP for different v_w values leads only to a maximum efficiency increase of less than 2%, the warped trajectories represent a very good approximation of their optimal counterparts. Therefore, it can be concluded that, in theory, warpage NMPC is a highly efficient algorithm for online generation of nearly optimal trajectories for the AWE system.

5.2. Implementation

After proving that the kite is a warpage system and that optimal (flying) trajectories can be obtained by warpage, the proposed warpage NMPC can be implemented in the AWE system. To evaluate the performance of the algorithm, the study will be divided into two parts: first, the controller will be analyzed using a simulator that regards the wind velocity as the only disturbance; this study provides the ideal improvements that can be obtained with the proposed controller. Then, in a second step, the analysis will be repeated considering a real plant simulator that includes all the real life disturbances; this second study provides the real improvements that can be obtained with the controller in real life conditions.

5.2.1. Initial assessment

As first assessment, the controller is tested under the assumption that wind velocity is the only disturbance. In particular, as depicted in Fig. 10, a realistic wind speed profile that drops in 25 min from 10 m/s to 6 m/s is considered.

Using the above profile, warpage NMPC is compared against a normal tracking NMPC scheme that uses a constant tracking trajectory

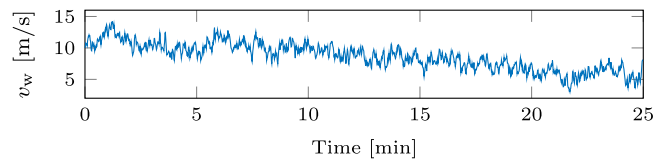


Fig. 10. Considered wind profile.

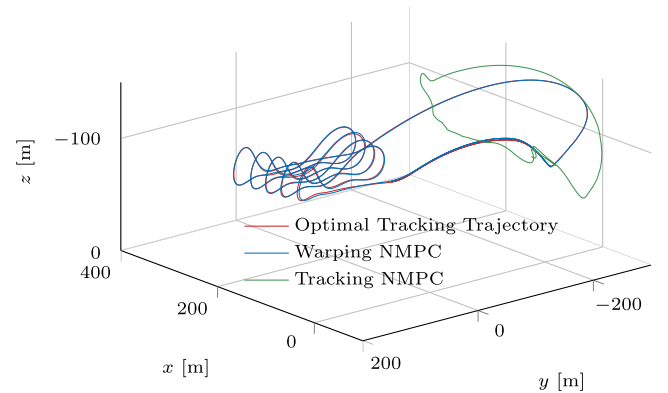


Fig. 11. Comparison between normal NMPC and warpage NMPC for $v_w = 6$ m/s in simulation environment.

Table 2

Efficiency comparison between warpage and tracking NMPC under the assumption that wind velocity is the only disturbance.

NMPC Scheme	η_{Loyd}
Tracking NMPC	-2.09%
Warping NMPC	31.57%

generated at $v_w = 10$ m/s. In particular, in order to evaluate the difference in performance when the wind speed is different from the one used when computing the reference trajectory, the two control schemes are evaluated at the end of wind speed profile interval ($v_w \approx 6$ m/s).

The comparison is illustrated in Fig. 11, which depicts the 3D pumping cycle trajectories at the end of the simulation interval, and Table 2, which compares the efficiency of the two control schemes in the last pumping cycle.

As it can be observed, the tracking NMPC scheme, which is based on a constant trajectory generated at $v_w = 10$ m/s, is unable to track the reference trajectory and extract energy (indicated by a negative Loyd factor $\eta_{Loyd} = -2.09\%$). In particular, it keeps the kite at a high elevation angle and barely performs any movement. By contrast, the warpage NMPC reaches power efficiencies ($\eta_{Loyd} = 31.57\%$) very close to the ideal one by adaptation to the varying wind speed v_w . Therefore, from these initial results, it seems clear warpage NMPC has the potential to greatly improve the efficiency of the AWE system.

5.2.2. Realistic plant simulator

To verify the results of the previous experiments, the analysis is repeated using a realistic plant simulator. In particular, the plant simulator developed by Skysails and whose equations of motion have been empirically validated with real flight data is employed. This plant simulation extends the wind speed disturbances to a complete set of real flight disturbances. In particular, considering the different effects observe in real flight conditions, the plant simulator includes the following disturbances:

1. Parameter mismatches to model that in real conditions the glide ratio E and the steering constant g_k are not the ideal estimated parameters.

Table 3

Warping NMPC comparison considering a nominal wind speed profile decrease from 10 m/s to 6 m/s.

NMPC Scheme	η_{Loyd}
Tracking NMPC	-3.41%
Warping NMPC	30.47%

2. A wind direction profile using real wind data.
3. An offset error on the control δ .
4. A realistic observer that makes estimation errors.
5. A delay between the steering command δ and its influence on the dynamic.

As before, the considered wind profile is the same as depicted in Fig. 10, i.e., a realistic wind speed profile that drops in 25 min from 10 m/s to 6 m/s. Likewise, the two control schemes are evaluated at the end of wind speed profile interval. The results are first listed in Table 3 where the efficiency of the two control schemes is compared. In addition, the 3D trajectories are again depicted in Fig. 12.

Considering the obtained results, the following observations can be made:

1. As before, due to the disturbances, tracking NMPC is unable to harvest any energy, i.e. it displays a negative efficiency.
2. By contrast, warping NMPC obtains an efficiency of 30.47%, which is very close to the ideal one obtained in the first assessment.
3. Warping NMPC not only obtains a good efficiency, but it is also able to keep the flying trajectories very close to the optimal one. In particular, by comparing Figs. 11 and 12 it can be observed that, while the real trajectories are now not as perfect as in the first assessment, warping NMPC manages to fly stable trajectories similar to the optimal ones despite being under real life disturbances.

Finally, to provide a more complete set of results, the comparison between tracking and warping NMPC in terms of the flying trajectories as a function of time is also included. In particular, Fig. 13 compares the flying trajectories of the state angles $[\psi, \varphi, \theta]^T$ for the two control schemes at the end of the wind profile interval. By observing the tremendous difference of performance in the three cases, it can be confirmed once again the importance of using warping NMPC in order to fly stable trajectories and to maximize the extracted energy.

5.3. Discussion

Considering the obtained results, there are 3 key topics that need further discussion: (1) the stability and efficiency of the proposed algorithm; (2) the effect of varying wind speeds within a single time period; (3) the computation time requirements of the proposed algorithm.

5.3.1. Stability and efficiency

When looking at the obtained results, it is clear that the proposed algorithm provides significant gains for the AWE system under study. In particular, while a regular version of tracking NMPC is unstable and unable to track flying trajectories, the proposed NMPC scheme can track optimal trajectories without any major issue.

Moreover, while the traditional tracking NMPC scheme is unable to harvest wind energy, the proposed scheme is able to harvest a significant amount of wind energy and obtain a Loyd efficiency that is very close to the maximum theoretical optimal efficiency.

5.3.2. Varying wind speeds

When analyzing the proposed algorithm, it is clear that one of its underlying assumptions is to consider a constant wind velocity during a

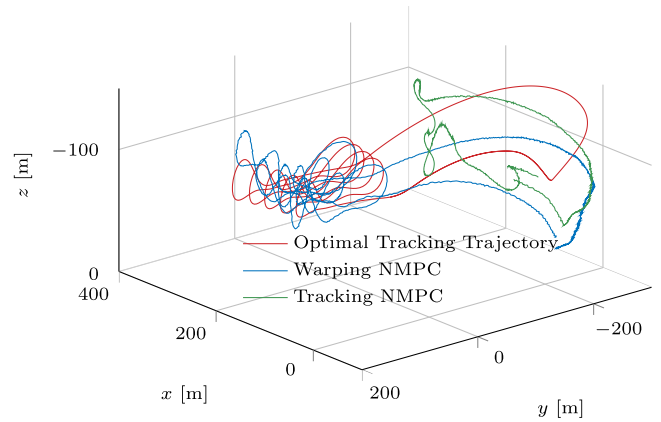


Fig. 12. Comparison between normal NMPC and warping NMPC in a real plant simulator.

time period. In particular, the tracking trajectory of the NMPC scheme is continuously updated considering the last position of the AWE system and the latest measurement of the wind speed. If the wind velocity does not change within a time period, this tracking trajectory is then guaranteed to be optimal.

As wind speed changes within a time period, a natural question to ask is whether the controller remains stable under this varying conditions and whether the trajectories remain optimal despite the changing wind speed.

From a stability point of view, it is clear that the algorithm can handle varying wind speeds. This can be shown considering the obtained results as, using a real simulator and varying wind conditions, the proposed algorithms keeps the AWE system stable and is able to track the trajectories without any issues.

From the point of view of optimality, it can be argued that the algorithm cannot track perfectly optimal trajectories as the assumption of constant wind speed does not hold. However, considering the stochastic nature of the wind speed, it can also be argued that assuming constant wind velocity is one of the best assumptions that can in practice be made to obtain optimal tracking trajectories. Moreover, considering that optimal trajectories have a Loyd efficiency of 33.7% and the proposed algorithm obtains (under real simulated conditions) an efficiency of 30.47%, it can further be argued that, while the tracking trajectories are not optimal, they are good enough for the controller to have a nearly optimal efficiency.

5.3.3. Computation time

One of the critical implementation considerations when using the proposed controller is whether its computation requirements are small enough for a real-time controller. Particularly, if a single algorithm iteration requires longer computation times than the controller sampling time, the proposed algorithm would not be suitable for running in real-time.

As warping is simply a scaling operation, its computation time is negligible compared to a NMPC iteration. Moreover, as the tracking NMPC solves a quadratic problem, the total computation time of a single iteration is much lower than the controller sampling time. In particular, using a standard 2016 laptop with an Intel i7-6920HQ CPU (quad core CPU with 2,9 GHz base frequency) and 16 GB of RAM, the iteration time is around 10 ms. Considering that the controller of the AWE system uses a sampling time of 100 ms, the proposed algorithm is suitable to run in real-time as the operational controller.

6. Conclusion

In this paper, the ideas of warping theory have been applied in order to build a NMPC algorithm that is able to perform online generation and tracking of optimal trajectories.

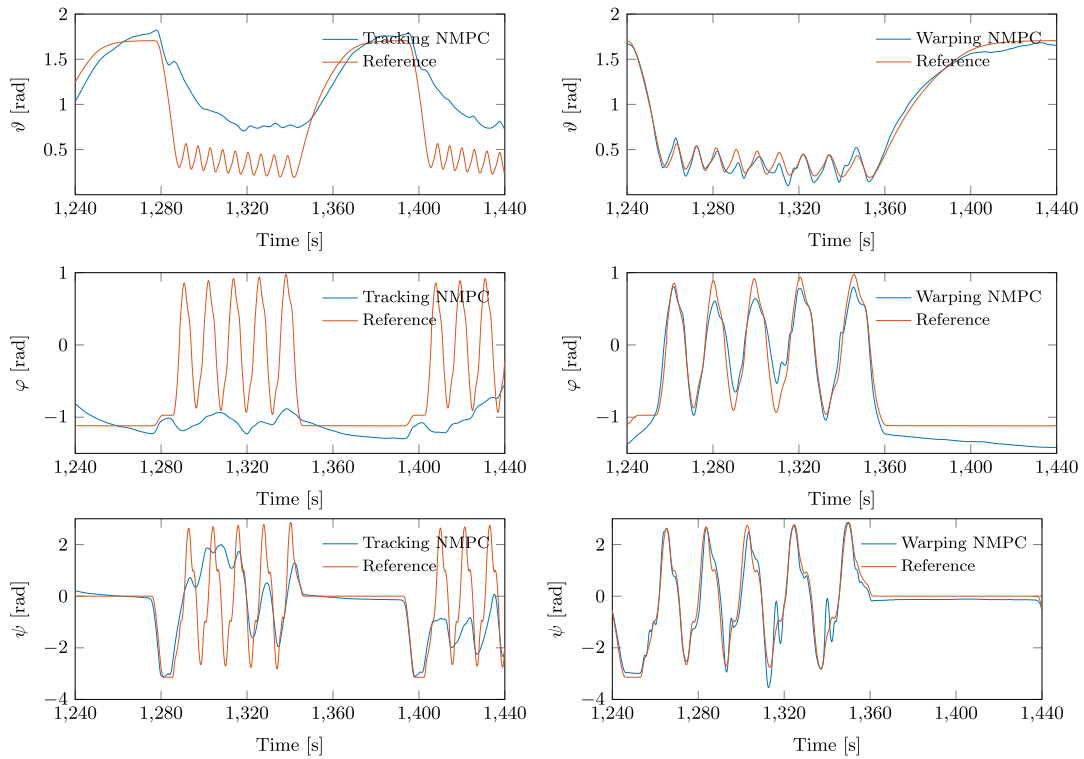


Fig. 13. Comparison between tracking and warping NMPC in terms of the trajectories of ψ , ϑ , and φ on the time domain. Left: tracking NMPC. Right: warping NMPC.

The algorithm, which is called warping NMPC, has been successfully implemented in the simulation framework of a real *airborne wind energy (AWE)*. In particular, the system under study has optimal trajectories that depend on the wind velocity v_w . As a result, to fly optimal trajectories and maximize the extracted energy, the control algorithm needs to re-adapt the flying trajectories in real-time. In this context, it has been shown how, using warping NMPC, the AWE system could keep the flying trajectories optimal, and in turn, double the extracted energy when compared with the previously proposed controller.

Acknowledgments

This research has received funding from the European Union’s Horizon 2020 research and innovation program under the Marie Skłodowska-Curie grant agreements No 675318 (INCITE), 642682 (AWESCO), and 607957 (TEMPO). In addition, it was also supported by the EU via ERC-HIGHWIND (259166) by the German Federal Ministry for Economic Affairs and Energy (BMWi) via eco4wind (0324125B) and DyConPV (0324166B) and by DFG in context of the Research Unit FOR 2401.

Appendix A. Warping theory

In this appendix, the conceptual explanations given in Section 3 are extended. In particular, the formal definition of the family of dynamical systems that can use warping is provided and a simple illustrative example is given. As it will be shown, the AWE system under study belongs to this class of systems, i.e. warpage systems. To formally define them, the notion of warped times frames needs to be first introduced.

A.1. Warped time frame τ

Consider a real time frame t which is used to describe any motion of a dynamical system. A *warped time frame* τ with respect to t can be defined by formulating the relation between the time velocities dt and $d\tau$

in both frames. This relation is called warping factor $\dot{w}(t)$ and is defined as:

$$\frac{d\tau}{dt} = \dot{w}(t),$$

with $\dot{w}(t) > 0$, $dt > 0$ and $d\tau > 0$. It is important to note that time transformations from t to τ can be computed by $\tau = w(t) = \int_0^t \dot{w}(t') dt'$. Likewise, τ can be warped back to obtain t by using $\frac{dt}{d\tau} = \frac{1}{\dot{w}(t)}$, i.e. the warping operation is bidirectional. According to these definitions, time is a strictly positive monotonic function, i.e. t and $\tau = w(t)$ must be strictly positive monotone.

Fig. A.14 exemplifies the relation between t and τ for different warping factors. In particular, the blue line represents the case where $\dot{w}(t)$ is constant and bigger than one which leads to a motion in the time frame τ relatively faster than in t . In contrast, the red line represents the opposite behavior, i.e. $\dot{w}(t)$ is still constant but the motion in t is now faster than in τ . Finally, the yellow line illustrates a general case where the warping factor varies as a function of time and the time variation in t with respect to τ is not constant.

A.2. Warpable dynamical system

Regard a general dynamical system defined by the EOM $\dot{\mathbf{x}}(t) = \Phi(\mathbf{x}(t), \mathbf{u}(t), p(t), t)$, with t representing the time, $\mathbf{x} \in \mathbb{R}^m$ the system state, $\mathbf{u} \in \mathbb{R}^n$ the system input, and $p \in \mathbb{R}$ the time dependent parameters. The system is defined as a *warpable dynamic system* if the EOM can be expressed as:

$$\begin{aligned} \dot{\mathbf{x}}(t) &= p(t) \mathbf{f}(\mathbf{x}(t), \mathbf{u}_1(t)) + \mathbf{L}(\mathbf{x}(t), \mathbf{u}_1(t)) \mathbf{u}_2(t) \\ &= p(t) \mathbf{g}(t) + \mathbf{S}(t) \mathbf{u}_2(t), \end{aligned} \quad (\text{A.1})$$

with : $p(t) \in \mathbb{R}$, $\mathbf{u}(t) = (\mathbf{u}_1(t), \mathbf{u}_2(t)) \in \mathbb{R}^{n_1+n_2}$,
 $\mathbf{f} : \mathbb{R}^{m+n_1} \rightarrow \mathbb{R}^m$, $\mathbf{L} : \mathbb{R}^{m+n_1} \rightarrow \mathbb{R}^{m \times n_2}$.

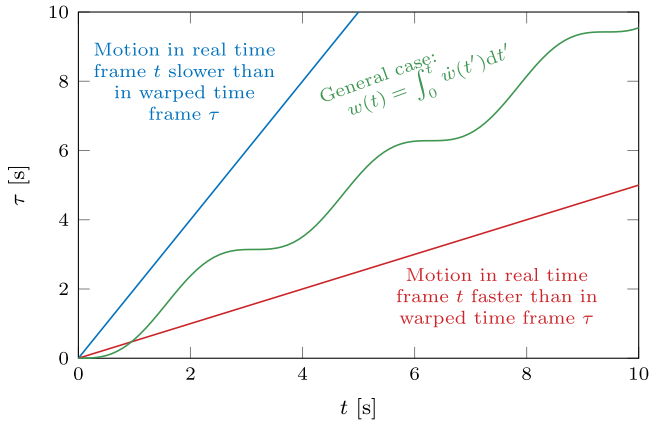


Fig. A.14. Warping factor and time variation in time frames τ , t . (For interpretation of the references to color in this figure legend, the reader is referred to the web version of this article.)

Lemma A.1 (Time Warped Dynamical System). Given the solution $(\mathbf{x}_{\text{ref}}(\tau), \mathbf{u}_{1,\text{ref}}(\tau), \mathbf{u}_{2,\text{ref}}(\tau))$ for a reference system:

$$\begin{aligned} \dot{\mathbf{x}}_{\text{ref}}(\tau) &= p_{\text{ref}} \mathbf{f}(\mathbf{x}_{\text{ref}}(\tau), \mathbf{u}_{1,\text{ref}}(\tau)) \\ &\quad + \mathbf{L}(\mathbf{x}_{\text{ref}}(\tau), \mathbf{u}_{1,\text{ref}}(\tau)) \mathbf{u}_{2,\text{ref}}(\tau) \\ &= p_{\text{ref}} \mathbf{g}_{\text{ref}}(\tau) + \mathbf{S}_{\text{ref}}(\tau) \mathbf{u}_{2,\text{ref}}(\tau), \end{aligned} \quad (\text{A.2})$$

a solution for the general system (A.1) is given by:

$$\mathbf{x}(t) = \mathbf{x}_{\text{ref}}(w(t)), \quad (\text{A.3a})$$

$$\mathbf{u}_1(t) = \mathbf{u}_{1,\text{ref}}(w(t)), \quad (\text{A.3b})$$

$$\mathbf{u}_2(t) = \dot{w}(t) \mathbf{u}_{2,\text{ref}}(w(t)), \quad (\text{A.3c})$$

where the warping factor between t and τ is defined by:

$$\dot{w}(t) = \frac{d\tau}{dt} = \frac{p(t)}{p_{\text{ref}}} \quad \text{and} \quad w(t) = \int_0^t \frac{p(t')}{p_{\text{ref}}} dt' = \tau. \quad (\text{A.4})$$

Note 1: without loss of generality, the initial condition $\mathbf{x}(0) = \mathbf{x}_{\text{ref}}(0)$ is assumed.

Note 2: a trajectory is assumed to be feasible as long as it respects the system dynamics, i.e. bounded trajectories are not considered.

Proof.

$$\begin{aligned} \dot{\mathbf{x}}(t) &\stackrel{(\text{A.3a})}{=} \left. \frac{d\mathbf{x}_{\text{ref}}}{d\tau} \right|_{\tau=w(t)} \dot{w}(t) \\ &\stackrel{(\text{A.2})}{=} \dot{w}(t) p_{\text{ref}} \mathbf{f}(\mathbf{x}_{\text{ref}}(w(t)), \mathbf{u}_{1,\text{ref}}(w(t))) \\ &\quad + \mathbf{L}(\mathbf{x}_{\text{ref}}(w(t)), \mathbf{u}_{1,\text{ref}}(w(t))) \dot{w}(t) \mathbf{u}_{2,\text{ref}}(w(t)) \\ &\stackrel{((\text{A.3a})-(\text{A.3c}))}{=} \stackrel{(\text{A.4})}{=} p(t) \mathbf{f}(\mathbf{x}(t), \mathbf{u}_1(t)) + \mathbf{L}(\mathbf{x}(t), \mathbf{u}_1(t)) \mathbf{u}_2(t). \quad \square \end{aligned} \quad (\text{A.5})$$

A.3. Warping interpretation

Time warping is a change on the velocity of the dynamics that bring a system to a different time frame. In this new time frame $\tau = w(t)$, the ratio $\dot{w}(t)$ between $p(t)$ and p_{ref} (ratio between $d\tau$ and dt) would characterize the ratio of the time velocities of the two time frames. An example of a motion in warped time frames can be given by the following system:

$$\begin{bmatrix} \dot{x}_1(t) \\ \dot{x}_2(t) \end{bmatrix} = \Omega(t) \begin{bmatrix} 0 & 1 \\ -1 & 0 \end{bmatrix} \begin{bmatrix} x_1(t) \\ x_2(t) \end{bmatrix} \quad (\text{A.6})$$

Considering $\Omega(t) = 1$ and $\mathbf{x}(0) = [1, 0]^T$, the solution reads $x_2(t) = \sin(t)$. Warping this solution with $\dot{w}(t) = 1/\Omega_2$, a trajectory $x_2(\tau) = \sin(\tau)$ in a time frame $\tau = t/\Omega_2$ is obtained. Fig. A.15 depicts these two trajectories for the case of $\Omega_2 = 2$.

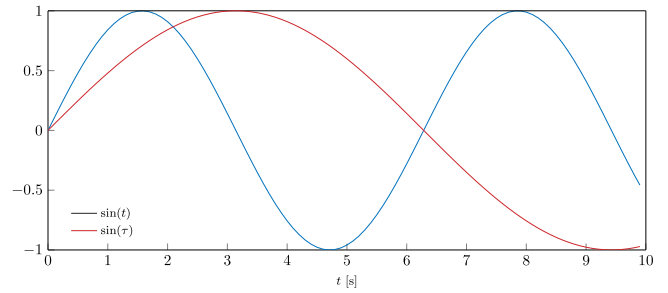


Fig. A.15. Warping of a sin trajectory with $\dot{w}(t) = \frac{1}{2}$.

In this warped time frame, $\mathbf{u}_{2,\text{ref}}(\tau) = \mathbf{u}_2(t)p_{\text{ref}}/p(t)$ is the set of inputs that not only have to be warped in time, but also amplified or attenuated to account for the $p(t)$ -independence of the second term of Eq. (A.1).

Appendix B. Optimality preservation in warping

In Appendix A, the notion of warped time frames, warpable systems, and warping trajectories was introduced. In this appendix, the theoretical foundations that explain that, for specific scenarios, warping preserves optimality are then presented.

B.1. Warpable optimal control problem

Regard a general *Optimal Control Problem (OCP)* defined in a time frame t :

$$\min_{\mathbf{y}(\cdot), T} J(\mathbf{y}(t)) = \int_0^T L(\mathbf{x}(t), \mathbf{u}(t), p(t)) dt \quad (\text{B.1a})$$

$$\text{s.t. } \Phi(\mathbf{x}(t), \mathbf{u}(t), p(t)) = \dot{\mathbf{x}}(t), \quad t \in [0, T] \quad (\text{B.1b})$$

$$\mathbf{h}(\mathbf{x}(t), \mathbf{u}(t)) \leq 0, \quad t \in [0, T] \quad (\text{B.1c})$$

$$\mathbf{r}(\mathbf{x}(0), \mathbf{x}(T)) \leq 0, \quad (\text{B.1d})$$

with

$$\mathbf{y}(t) = (\mathbf{x}(t), \mathbf{u}(t)). \quad (\text{B.1e})$$

The general OCP is defined to be a *Warpable Optimal Control Problem (WOCP)* if it holds that:

1. The dynamical system of the OCP is warpable:

$$\Phi(\cdot) = p(t) \mathbf{f}(\mathbf{x}(t), \mathbf{u}_1(t)) + \mathbf{L}(\mathbf{x}(t), \mathbf{u}_1(t)) \mathbf{u}_2(t). \quad (\text{B.2a})$$

2. $p(t) \in \mathbb{R}_{++}$ is constant in the time interval $[0, T]$.

3. The path constraints are independent of $\mathbf{u}_2(t)$:

$$\mathbf{h}(\mathbf{x}(t), \mathbf{u}(t)) = \mathbf{h}(\mathbf{x}(t), \mathbf{u}_1(t)). \quad (\text{B.2b})$$

4. The cost of the OCP can be written as:

$$\int_0^T L_1(p) L_2\left(\mathbf{x}(t), \mathbf{u}_1(t), \frac{\mathbf{u}_2(t)}{p}\right) dt. \quad (\text{B.2c})$$

In this case, a WOCP is equal to:

WOCP(p):

$$\min_{\mathbf{y}(\cdot), T} \int_0^T L_1(p) L_2\left(\mathbf{x}(t), \mathbf{u}_1(t), \frac{\mathbf{u}_2(t)}{p}\right) dt \quad (\text{B.3a})$$

$$\text{s.t. } p \mathbf{g}(t) + \mathbf{S}(t) \mathbf{u}_2(t) = \dot{\mathbf{x}}(t), \quad t \in [0, T] \quad (\text{B.3b})$$

$$\mathbf{h}(\mathbf{x}(t), \mathbf{u}_1(t)) \leq 0, \quad t \in [0, T] \quad (\text{B.3c})$$

$$\mathbf{r}(\mathbf{x}(0), \mathbf{x}(T)) \leq 0. \quad (\text{B.3d})$$

Theorem B.1 (Optimality of Warpable Dynamical Systems). *Regard the WOCP in a reference time frame:*

$$\begin{aligned} \min_{\mathbf{y}_{\text{ref}}(\cdot), \bar{\tau}} \int_0^{\bar{\tau}} L_1(p_{\text{ref}}) L_2 \left(\mathbf{x}_{\text{ref}}(\tau), \mathbf{u}_{1,\text{ref}}(\tau), \frac{\mathbf{u}_{2,\text{ref}}(\tau)}{p_{\text{ref}}} \right) d\tau \quad (\text{B.4}) \\ \text{s.t. } p_{\text{ref}} \mathbf{g}_{\text{ref}}(\tau) + \mathbf{S}_{\text{ref}}(\tau) \mathbf{u}_{2,\text{ref}}(\tau) = \dot{\mathbf{x}}_{\text{ref}}(\tau), \quad \tau \in [0, \bar{\tau}] \\ \mathbf{h}(\mathbf{x}_{\text{ref}}(\tau), \mathbf{u}_{1,\text{ref}}(\tau)) \leq 0, \quad \tau \in [0, \bar{\tau}] \\ \mathbf{r}(\mathbf{x}_{\text{ref}}(0), \mathbf{x}_{\text{ref}}(\bar{\tau})) \leq 0. \end{aligned}$$

Given the optimal solution of the reference problem:

$$\mathbf{y}_{\text{ref}}^*(\tau) = (\mathbf{x}_{\text{ref}}^*(\tau), \mathbf{u}_{1,\text{ref}}^*(\tau), \mathbf{u}_{2,\text{ref}}^*(\tau)), \quad (\text{B.5})$$

then, the warped trajectory of $\mathbf{y}_{\text{ref}}^*(\tau)$:

$$\mathbf{y}_p(t) = (\mathbf{x}_p(t), \mathbf{u}_{p1}(t), \mathbf{u}_{p2}(t)), \quad (\text{B.6})$$

with constant warping factor:

$$\dot{w}(t) = \frac{p}{p_{\text{ref}}} = \dot{w}, \quad (\text{B.7})$$

and with warping transformations defined by (A.3a)–(A.3c), is the optimal solution of (B.3), i.e.:

$$\mathbf{x}_p(t) := \mathbf{x}_{\text{ref}}^*(w(t)) = \mathbf{x}_{\text{ref}}^*(t), \quad (\text{B.8a})$$

$$\mathbf{u}_{p1}(t) := \mathbf{u}_{1,\text{ref}}^*(w(t)) = \mathbf{u}_{1,\text{ref}}^*(t), \quad (\text{B.8b})$$

$$\mathbf{u}_{p2}(t) := \mathbf{u}_{2,\text{ref}}^*(w(t)) \dot{w} = \mathbf{u}_{2,\text{ref}}^*(t). \quad (\text{B.8c})$$

Note that, since the warping factor is time independent, time warping becomes a linear transformation:

$$\tau = \int_0^t \frac{p}{p_{\text{ref}}} dt' = \frac{p}{p_{\text{ref}}} t \implies \bar{\tau} = w(T) = \frac{p}{p_{\text{ref}}} T. \quad (\text{B.9})$$

Proof. If $\mathbf{y}_{\text{ref}}^*(\tau)$ is defined as the solution of:

$$\min_{\mathbf{y}_{\text{ref}}(\cdot), \bar{\tau}} \int_0^{\bar{\tau}=w(T)} L_1(p_{\text{ref}}) L_2 \left(\mathbf{x}_{\text{ref}}(\tau), \mathbf{u}_{1,\text{ref}}(\tau), \frac{\mathbf{u}_{2,\text{ref}}(\tau)}{p_{\text{ref}}} \right) d\tau \quad (\text{B.10a})$$

$$p_{\text{ref}} \mathbf{g}_{\text{ref}}(\tau) + \mathbf{S}_{\text{ref}}(\tau) \mathbf{u}_{2,\text{ref}}(\tau) = \dot{\mathbf{x}}_{\text{ref}}(\tau), \quad \tau \in [0, \bar{\tau}], \quad (\text{B.10b})$$

$$\mathbf{h}(\mathbf{x}_{\text{ref}}(\tau), \mathbf{u}_{1,\text{ref}}(\tau)) \leq 0, \quad \tau \in [0, \bar{\tau}], \quad (\text{B.10c})$$

$$\mathbf{r}(\mathbf{x}_{\text{ref}}(0), \mathbf{x}_{\text{ref}}(\bar{\tau})) \leq 0, \quad (\text{B.10d})$$

then, by (A.4) and (B.9), and moving the constant terms out of the integral, it holds that $\mathbf{y}_{\text{ref}}^*(\tau)$ is also the solution of:

$$\min_{\mathbf{y}_{\text{ref}}(\cdot), T} L_1(p_{\text{ref}}) \int_0^T L_2 \left(\mathbf{x}_{\text{ref}}(w(t)), \mathbf{u}_{1,\text{ref}}(w(t)), \frac{\mathbf{u}_{2,\text{ref}}(w(t))}{p_{\text{ref}}} \right) \dot{w} dt \quad (\text{B.11a})$$

s.t.

$$p_{\text{ref}} \mathbf{g}_{\text{ref}}(w(t)) + \mathbf{S}_{\text{ref}}(w(t)) \mathbf{u}_{2,\text{ref}}(w(t)) = \dot{\mathbf{x}}_{\text{ref}}(w(t)), \quad \frac{p}{p_{\text{ref}}} t \in [0, \frac{p}{p_{\text{ref}}} T], \quad (\text{B.11b})$$

$$\mathbf{h}(\mathbf{x}_{\text{ref}}(w(t)), \mathbf{u}_{1,\text{ref}}(w(t))) \leq 0, \quad \frac{p}{p_{\text{ref}}} t \in [0, \frac{p}{p_{\text{ref}}} T], \quad (\text{B.11c})$$

$$\mathbf{r}(\mathbf{x}_{\text{ref}}(w(0)), \mathbf{x}_{\text{ref}}(w(T))) \leq 0. \quad (\text{B.11d})$$

Then, considering the warping relations (A.3a)–(A.3c) and (A.5), and defining $\mathbf{y}_p(t)$ as the warped version of $\mathbf{y}_{\text{ref}}^*(\tau)$, it also holds that $\mathbf{y}_p(t)$ is

the optimal solution of:

$$\min_{\mathbf{y}(\cdot), T} L_1(p_{\text{ref}}) \int_0^T L_2 \left(\mathbf{x}(t), \mathbf{u}_1(t), \frac{\mathbf{u}_2(t)}{\dot{w} p_{\text{ref}}} \right) \dot{w} dt \quad (\text{B.12a})$$

$$\text{s.t. } \frac{p \mathbf{g}(t) + \mathbf{S}(t) \mathbf{u}_2(t)}{\dot{w}} = \frac{\dot{\mathbf{x}}(t)}{\dot{w}}, \quad t \in [0, T], \quad (\text{B.12b})$$

$$\mathbf{h}(\mathbf{x}(t), \mathbf{u}_1(t)) \leq 0, \quad t \in [0, T], \quad (\text{B.12c})$$

$$\mathbf{r}(\mathbf{x}(0), \mathbf{x}(T)) \leq 0. \quad (\text{B.12d})$$

Next, by the definition (B.7) of the warping factor \dot{w} and reformulating $L_1(p_{\text{ref}})$ as $\frac{L_1(p_{\text{ref}}) L_1(p)}{L_1(p)}$, it follows that $\mathbf{y}_p(t)$ is also the optimal solution of:

$$\min_{\mathbf{y}(\cdot), T} \frac{p L_1(p_{\text{ref}})}{p_{\text{ref}} L_1(p)} \int_0^T L_1(p) L_2 \left(\mathbf{x}(t), \mathbf{u}_1(t), \frac{\mathbf{u}_2(t)}{p} \right) dt \quad (\text{B.13a})$$

$$\text{s.t. } p \mathbf{g}(t) + \mathbf{S}(t) \mathbf{u}_2(t) = \dot{\mathbf{x}}(t), \quad t \in [0, T], \quad (\text{B.13b})$$

$$\mathbf{h}(\mathbf{x}(t), \mathbf{u}_1(t)) \leq 0, \quad t \in [0, T], \quad (\text{B.13c})$$

$$\mathbf{r}(\mathbf{x}(0), \mathbf{x}(T)) \leq 0. \quad (\text{B.13d})$$

Finally, as a constant factor multiplying the cost function does not change the optimal solution of the OCP, $\mathbf{y}_p(t)$, the warped version of $\mathbf{y}_{\text{ref}}^*(\tau)$, must also be the optimal solution of the original problem:

$$\min_{\mathbf{y}(\cdot), T} \int_0^T L_1(p) L_2 \left(\mathbf{x}(t), \mathbf{u}_1(t), \frac{\mathbf{u}_2(t)}{p} \right) dt \quad (\text{B.14a})$$

$$\text{s.t. } p \mathbf{g}(t) + \mathbf{S}(t) \mathbf{u}_2(t) = \dot{\mathbf{x}}(t), \quad t \in [0, T], \quad (\text{B.14b})$$

$$\mathbf{h}(\mathbf{x}(t), \mathbf{u}_1(t)) \leq 0, \quad t \in [0, T], \quad (\text{B.14c})$$

$$\mathbf{r}(\mathbf{x}(0), \mathbf{x}(T)) \leq 0. \quad \square \quad (\text{B.14d})$$

B.2. Semi-Warpable optimal control problem

Consider a general WOCP as given by (B.3a)–(B.3d). The problem extension of adding $\mathbf{u}_2(t)$ -dependent path constraints is defined as *Semi-Warpable Optimal Control Problem (SWOCP)* and can be expressed as:

SWOCP(p):

$$\min_{\mathbf{y}(\cdot)} \int_0^T L_1(p) L_2 \left(\mathbf{x}(t), \mathbf{u}_1(t), \frac{\mathbf{u}_2(t)}{p} \right) dt \quad (\text{B.15a})$$

s.t.

$$p \mathbf{g}(t) + \mathbf{S}(t) \mathbf{u}_2(t) = \dot{\mathbf{x}}(t), \quad t \in [0, T] \quad (\text{B.15b})$$

$$\mathbf{h}(\mathbf{x}(t), \mathbf{u}_1(t)) \leq 0, \quad t \in [0, T] \quad (\text{B.15c})$$

$$\mathbf{h}_2(\mathbf{x}(t), \mathbf{u}_1(t), \mathbf{u}_2(t)) \leq 0 \quad t \in [0, T] \quad (\text{B.15d})$$

$$\mathbf{r}(\mathbf{x}(0), \mathbf{x}(T)) \leq 0. \quad (\text{B.15e})$$

It is important to note that, by adding \mathbf{u}_2 -dependent constraints, a warped version \mathbf{y}_p of an optimal reference trajectory $\mathbf{y}_{\text{ref}}^*(\tau)$ does not necessarily satisfy feasibility:

$$\mathbf{h}_2(\mathbf{x}_{\text{ref}}^*(\tau), \mathbf{u}_{1,\text{ref}}^*(\tau), \mathbf{u}_{2,\text{ref}}^*(\tau)) \leq 0$$

$$\implies \mathbf{h}_2(\mathbf{x}_p(t), \mathbf{u}_{p1}(t), \frac{p_{\text{ref}}}{p} \mathbf{u}_{p2}(t)) \leq 0$$

$$\not\Rightarrow \mathbf{h}_2(\mathbf{x}_p(t), \mathbf{u}_{p1}(t), \mathbf{u}_{p2}(t)) \leq 0. \quad (\text{B.16})$$

Definition B.1 (Warpable Reference (WR)). Regard a general warpable system with $p \in [p_{\min}, p_{\max}]$. Consider as well general inequality constraints

$$\mathbf{h}_2(\mathbf{x}(t), \mathbf{u}_1(t), \mathbf{u}_2(t)) \leq 0, \quad t \in [0, T], \quad (\text{B.17})$$

that any feasible trajectory should satisfy. Then, the trajectory $\mathbf{y}_{wr}(t)$, obtained for a parameter value p_{wr} , is defined to be a *warpable reference (WR)* if:

1. $\mathbf{y}_{wr}(t)$ satisfies (B.17).
2. Any warped trajectory of $\mathbf{y}_{wr}(t)$, with warping factor $\dot{w} = p/p_{wr}$, satisfies (B.17).

Definition B.2 (Best Warpable Reference (BWR)). Regard a general SWOCP as defined by (B.15b) and with $p \in [p_{min}, p_{max}]$. A trajectory $\mathbf{y}_{bwr}(t)$, obtained for a parameter value p_{bwr} , is defined to be a *best warpable reference (BWR)* if:

1. $\mathbf{y}_{bwr}(t)$ is an optimal solution of the SWOCP(p_{bwr}).
2. $\mathbf{y}_{bwr}(t)$ is a WR with respect to the constraint (B.17).

Corollary B.1 (Optimal Reference for SWOCP). Regard a SWOCP for which a BWR exists and the constraint (B.15d) is inactive at this BWR. Then, the BWR could be regarded as an optimal reference, i.e. $p_{ref} = p_{bwr}$, and any warped trajectory $\mathbf{y}_p(t)$, obtained by warping the optimal solution $\mathbf{y}_{ref}^*(\tau)$ of the reference SWOCP(p_{ref}) = SWOCP(p_{bwr}), is also an optimal solution of the general SWOCP(p).

Proof. In an optimization problem, any inactive inequality constraint at the optimal solution can be removed from the problem without modifying the local optimal solution (global in case of convex problems). In our case, the \mathbf{u}_2 -dependent constraint (B.15d) is inactive at $\mathbf{y}_{ref}^*(\tau)$ and by Definitions B.1 and B.2 any warped trajectory $\mathbf{y}_p(t)$ also satisfies (B.15d). As a result, (B.15d) can be removed, the original SWOCP is transformed into a WOC and Corollary B.1 holds directly due to Theorem B.1. \square

Remark. If \mathbf{h}_2 is active for p_{bwr} , i.e. $\mathbf{h}_2(\mathbf{y}_{bwr}(\tau)) = 0$, the warped trajectories $\mathbf{y}_p(t)$ are usually suboptimal. In this case, since they are still feasible and are generated from an optimal trajectory, they still represent a better solution than a random feasible trajectory.

Theorem B.2 (Existence and Generation of BWRs). Regard the optimal solution of the SWOCP(p_{max}) to be $\mathbf{y}_{max}^*(\tau)$. Regard as well m inequality constraints involving \mathbf{u}_2 , i.e. $\mathbf{h}_2(\mathbf{x}, \mathbf{u}_1, \mathbf{u}_2) = [h_{2,1}(\cdot), h_{2,2}(\cdot), \dots, h_{2,m}(\cdot)]$. If $h_{2,i}(\mathbf{x}(\tau), \mathbf{u}_1(\tau), \mathbf{u}_2(\tau))$, $\forall i = 1, \dots, m$ and $\forall \tau \in [0, \bar{\tau}]$, is monotonically increasing (decreasing) with respect to \mathbf{u}_2 and is only active for $\mathbf{u}_2 \geq 0$ ($\mathbf{u}_2 \leq 0$), then $\mathbf{y}_{max}^*(\tau)$ is a BWR.

Proof. Since $\mathbf{y}_{p_{max}}^*(\tau)$ is an optimal solution, it satisfies the constraint $h_{2,i}(\cdot) \leq 0$. Furthermore, using the standard warping relations (B.8a)–(B.8c), feasibility is equivalent to saying that any warped trajectory $\mathbf{y}_p(t)$ satisfies:

$$h_{2,i}(\mathbf{x}_p(t), \mathbf{u}_{p1}(t), \frac{p_{max}}{p} \mathbf{u}_{p2}(t)) \leq 0. \tag{B.18}$$

Moreover, for any monotonically increasing (decreasing) $h_{2,i}$ and positive (negative) values of \mathbf{u}_2 it holds that:

$$h_{2,i}(\mathbf{x}_p(t), \mathbf{u}_{p1}(t), \mathbf{u}_{p2}(t)) \leq h_{2,i}(\mathbf{x}_p(t), \mathbf{u}_{p1}(t), \frac{p_{max}}{p} \mathbf{u}_{p2}(t)) \tag{B.19}$$

Finally, combining (B.18)–(B.19) and using the fact that \mathbf{h}_2 is only active for positive (negative) \mathbf{u}_2 values, it holds that:

$$h_{2,i}(\mathbf{x}_p(t), \mathbf{u}_{p1}(t), \mathbf{u}_{p2}(t)) \leq 0. \tag{B.20}$$

As a result, any warped trajectory $\mathbf{y}_p(t)$ is a feasible solution with respect to $h_{2,i}(\cdot)$, $\forall i = 1, \dots, m$, and $\mathbf{y}_{p_{max}}^*(\tau)$ is a BWR. \square

Corollary B.2. An important class of functions satisfying the above equations is any $\mathbf{h}_2(\mathbf{x}(t), \mathbf{u}_1(t), \mathbf{u}_2(t))$ that can be reformulated as:

$$\mathbf{f}_{lower}(\mathbf{x}(t), \mathbf{u}_1(t)) \leq \mathbf{u}_2(t) \leq \mathbf{f}_{upper}(\mathbf{x}(t), \mathbf{u}_1(t)), \tag{B.21}$$

where : $\mathbf{f}_{lower}(\mathbf{x}, \mathbf{u}_1) < 0$, $\mathbf{f}_{upper}(\mathbf{x}, \mathbf{u}_1) > 0$.

Proof. The above constraint is equivalent to:

$$\mathbf{u}_2(t) - \mathbf{f}_{upper}(\mathbf{x}(t), \mathbf{u}_1(t)) \leq 0, \tag{B.22a}$$

$$-\mathbf{u}_2(t) + \mathbf{f}_{lower}(\mathbf{x}(t), \mathbf{u}_1(t)) \leq 0, \tag{B.22b}$$

and this reformulation satisfies the conditions of Theorem B.2 as:

1. (B.22a) is monotonically increasing with respect to \mathbf{u}_2 and, since $\mathbf{f}_{upper}(\mathbf{x}, \mathbf{u}_1) > 0$, it can only be active for $\mathbf{u}_2 > 0$.
2. (B.22b) is monotonically decreasing with respect to \mathbf{u}_2 and it can only be active for $\mathbf{u}_2 < 0$.
3. Only one of the two equations can be active at the same time as (B.22a) is active for $\mathbf{u}_2 > 0$ and (B.22b) is active for $\mathbf{u}_2 < 0$. \square

It should be finally mentioned, that there are SWOCPs, for which no BWR exists. As this is not the case for the AWE system under study, the applicability of warping to those kinds of SWOCPs is far beyond the scope of this paper.

References

Ahrens, U., Diehl, M., & Schmehl, R. (Eds.). (2013). *Airborne wind energy*. Springer-Verlag Berlin Heidelberg.

Alexis, K., Nikolakopoulos, G., & Tzes, A. (2014). On trajectory tracking model predictive control of an unmanned quadrotor helicopter subject to aerodynamic disturbances. *Asian Journal of Control*, 16(1), 209–224. <http://dx.doi.org/10.1002/asjc.587>.

Andersson, J. (2013). *A general-purpose software framework for dynamic optimization* (Ph.D. thesis), K.U. Leuven.

Bock, H. G., & Plitt, K. J. (1984). A multiple shooting algorithm for direct solution of optimal control problems. In *Proceedings of the IFAC world congress* (pp. 242–247). Pergamon Press.

Chauhdry, M., & Luh, P. (2012). Nested partitions for global optimization in nonlinear model predictive control. *Control Engineering Practice*, 20(9), 869–881. <http://dx.doi.org/10.1016/j.conengprac.2012.05.003>.

Cortinovis, A., Mercangöz, M., Mathur, T., Poland, J., & Blaumann, M. (2013). Nonlinear coal mill modeling and its application to model predictive control. *Control Engineering Practice*, 21(3), 308–320. <http://dx.doi.org/10.1016/j.conengprac.2012.10.006>.

Dutta, A., Depaetere, B., Ionescu, C., Pinte, G., Swevers, J., & De, K. (2014). Comparison of two-level NMPC and ILC strategies for wet-clutch control. *Control Engineering Practice*, 22(1), 114–124. <http://dx.doi.org/10.1016/j.conengprac.2013.10.003>.

Erhard, M., Horn, G., & Diehl, M. (2017). A quaternion-based model for optimal control of an airborne wind energy system. *ZAMM - Journal of Applied Mathematics and Mechanics*, 97(1), 7–24.

Erhard, M., & Strauch, H. (2013a). Control of towing kites for seagoing vessels. *IEEE Transactions on Control Systems Technology*, 21(5), 1629–1640. <http://dx.doi.org/10.1109/TCST.2012.2221093>.

Erhard, M., & Strauch, H. (2013b). Theory and experimental validation of a simple comprehensible model of tethered kite dynamics used for controller design. In *Airborne Wind Energy* (pp. 141–165). Springer.

Erhard, M., & Strauch, H. (2015). Flight control of tethered kites in autonomous pumping cycles for airborne wind energy. *Control Engineering Practice*, 40, 13–26. <http://dx.doi.org/10.1016/j.conengprac.2015.03.001>.

Fagiano, L., Milanese, M., & Piga, D. (2012). Optimization of airborne wind energy generators. *International Journal of Robust and Nonlinear Control*, 22(18), 2055–2083. <http://dx.doi.org/10.1002/rnc.1808>.

Gros, S., Zanon, M., & Diehl, M. (2013). A relaxation strategy for the optimization of airborne wind energy systems. In *Proceedings of the European control conference* (pp. 1011–1016).

Grüne, L., & Pannek, J. (2011). *Nonlinear model predictive control*. London: Springer.

Guerreiro, B. J., Silvestre, C., Cunha, R., & Pascoal, A. (2014). Trajectory tracking nonlinear model predictive control for autonomous surface craft. *IEEE Transactions on Control Systems Technology*, 22(6), 2160–2175. <http://dx.doi.org/10.1109/TCST.2014.2303805>.

Lago, J., Erhard, M., & Diehl, M. (2017). Warping NMPC for online generation and tracking of optimal trajectories. *IFAC-PapersOnLine*, 50(1), 13252–13257. <http://dx.doi.org/10.1016/j.ifacol.2017.08.1961>.

Lago, J. (2016). *Periodic optimal control and model predictive control of a tethered kite for airborne wind energy* (Master's thesis), University of Freiburg.

Loyd, M. (1980). Crosswind kite power. *Journal of Energy*, 4(3), 106–111.

Nagy, Z., Mahn, B., Franke, R., & Allgöwer, F. (2007). Evaluation study of an efficient output feedback nonlinear model predictive control for temperature tracking in an industrial batch reactor. *Control Engineering Practice*, 15(7), 839–850. <http://dx.doi.org/10.1016/j.conengprac.2006.05.004>.

- Rawlings, J. B., & Amrit, R. (2009). Optimizing process economic performance using model predictive control. In *Nonlinear model predictive control: Towards new challenging applications* (pp. 119–138). Berlin Heidelberg: Springer.
- Wächter, A., & Biegler, L. T. (2006). On the implementation of an interior-point filter line-search algorithm for large-scale nonlinear programming. *Mathematical Programming*, 106(1), 25–57.
- Wiese, A., Blom, M., Manzie, C., Brear, M., & Kitchener, A. (2015). Model reduction and mimo model predictive control of gas turbine systems. *Control Engineering Practice*, 45, 194–206. <http://dx.doi.org/10.1016/j.conengprac.2015.09.015>.
- Zanon, M., Gros, S., & Diehl, M. (2016). A tracking MPC formulation that is locally equivalent to economic MPC. *Journal of Process Control*, 45, 30–42. <http://dx.doi.org/10.1016/j.jprocont.2016.06.006>.